Introduction and removal of hydroxyl groups in vitreous silica

Citation for published version (APA):
vd Steen, G. H. A. M. (1976). *Introduction and removal of hydroxyl groups in vitreous silica*. [Phd Thesis 1 (Research TU/e / Graduation TU/e), Chemical Engineering and Chemistry]. Technische Hogeschool Eindhoven. https://doi.org/10.6100/IR76787

DOI:
10.6100/IR76787

Document status and date:
Published: 01/01/1976

Document Version:
Publisher's PDF, also known as Version of Record (includes final page, issue and volume numbers)

Please check the document version of this publication:

• A submitted manuscript is the version of the article upon submission and before peer-review. There can be important differences between the submitted version and the official published version of record. People interested in the research are advised to contact the author for the final version of the publication, or visit the DOI to the publisher's website.
• The final author version and the galley proof are versions of the publication after peer review.
• The final published version features the final layout of the paper including the volume, issue and page numbers.

Link to publication

General rights
Copyright and moral rights for the publications made accessible in the public portal are retained by the authors and/or other copyright owners and it is a condition of accessing publications that users recognise and abide by the legal requirements associated with these rights.

- Users may download and print one copy of any publication from the public portal for the purpose of private study or research.
- You may not further distribute the material or use it for any profit-making activity or commercial gain
- You may freely distribute the URL identifying the publication in the public portal.

If the publication is distributed under the terms of Article 25fa of the Dutch Copyright Act, indicated by the "Taverne" license above, please follow below link for the End User Agreement:

www.tue.nl/taverne

Take down policy
If you believe that this document breaches copyright please contact us at:

openaccess@tue.nl

providing details and we will investigate your claim.

Download date: 04. Oct. 2023

INTRODUCTION AND REMOVAL OF HYDROXYL GROUPS IN VITREOUS SILICA

G. H. A. M. VAN DER STEEN

INTRODUCTION AND REMOVAL OF HYDROXYL GROUPS IN VITREOUS SILICA

PROEFSCHRIFT

TER VERKRIJGING VAN DE GRAAD VAN DOCTOR IN DE TECHNISCHE WETENSCHAPPEN AAN DE TECHNISCHE HOGESCHOOL EINDHOVEN, OP GEZAG VAN DE RECTOR MAGNIFICUS, PROF. DR. IR. G. VOSSERS, VOOR EEN COMMISSIE AANGEWEZEN DOOR HET COLLEGE VAN DEKANEN IN HET OPENBAAR TE VERDEDIGEN OP 6 APRIL 1976 TE 16.00 UUR

DOOR

GERARDUS HENRICUS ANTONIUS MARIA
VAN DER STEEN

GEBOREN TE TILBURG

DIT PROEFSCHRIFT IS GOEDGEKEURD DOOR DE PROMOTOREN
PROF. DR. J. M. STEVELS EN PROF. DR. G. C. A. SCHUIT

Aan Marga
Aan mijn ouders

Dankbetuiging

De leiding van het Ontwikkelingscentrum Glas van de N.V. Philips' Gloeilampenfabrieken, Dr. W. Verweij en Dr. Ir. A. Kats, ben ik erkentelijk voor de toestemming om het onderzoek aan kwartsglazen te verrichten en de resultaten te publiceren.

Voor de uitvoering van de vele experimenten wil ik in het bijzonder P. van der Ree, C. D. J. C. de Laat, J. J. van de Geer en W. F. Albersen bedanken, alsmede de medewerkers van het Ontwikkelingscentrum Glas, die aan het onderzoek hebben bijgedragen.

Ing. H. van den Boom ben ik dank verschuldigd voor de nauwe samenwerking tijdens het Raman onderzoek.

Met Dr. D. J. Breed, Dr. E. Papanikolau en Ir. A. P. Vervaart had ik veel uitvoerige discussies die resulteerden in een aantal goede suggesties.

Dank ben ik verschuldigd aan Dr. D. J. Breed, Dr. R. G. Gossink, Dr. F. Meyer, Dr. A. Kats, Ir. A. P. Vervaart, Ir. J. van Lieshout en Dr. W. L. Konijnendijk voor het kritisch doorlezen van de manuscripten.

CONTENTS

EXPERIMENTAL WORK

INTRODUCTION

One of the main applications of vitreous silica is found in the lamp industries. Lamps operating at particularly high temperature, such as gas discharge and halogen lamps, have vitreous silica envelopes.

The high softening point and chemical resistance of the glass are the favourable properties which are utilised. Although silicon dioxide is chemically inert with respect to a wide range of materials and compounds even at high temperatures, the gases which are most commonly dissolved in the glass (H_2 and H_2O) are not.

In gas discharge lampes, for example, water will react with the molybdenum or tungsten electrodes and hydrogen will increase the ignition voltage of the lamp. In halogen lamps hydrogen and water will participate in the halogen cycle and affect the resistance wire.

Most industrial melting processes make use of hydrogen-containing gas mixtures (e.g. N_2-H_2 mixtures) in order to protect the materials (Mo en W) from which most melting crucibles are made. It is inevitable therefore that hydrogen is introduced into the glass during melting.

Some processes are known which directly use the high solubility of hydrogen (and He) in vitreous silica. During melting the hydrogen and helium dissolve in the glass and a bubble free vitreous silica is obtained.

For the above reasons it is important to know about the behaviour of hydrogen in the glass. The system H_2-SiO_2 is also interesting from a scientific point of view. The system is in fact one of the few systems making it relatively easy to study gas, solid-state reactions.

SUMMARY

The chronological sequence in which the investigations were made is more or less the same as the sequence in which the papers bundled in this thesis were published.

The more data that became available, the easier it was to define the chemical systems and processes and the easier it was to select the kind of experiments needed to check the validity of the models. In this summary we shall proceed in the reverse order. Firstly the systems will be defined, and the validity of the models will be demonstrated with the aid of the experimental results.

Reactions between hydrogen and vitreous silica

Hydrogen reacts with vitreous silica according to a mechanism of which the net result will be as follows:

$$\underset{\text{glass}}{2\,SiO_2} + \underset{\text{gas}}{H_2} \underset{K_2}{\overset{K_1}{\rightleftarrows}} \equiv SiOH + \equiv SiH \qquad (1)$$

where

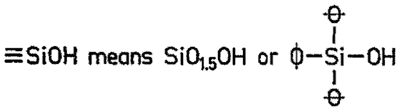

$$\equiv SiOH \text{ means } SiO_{1.5}OH \text{ or } \Phi-\overset{\overset{\Theta}{|}}{\underset{\underset{\Theta}{|}}{Si}}-OH$$

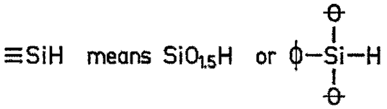

$$\equiv SiH \text{ means } SiO_{1.5}H \text{ or } \Phi-\overset{\overset{\Theta}{|}}{\underset{\underset{\Theta}{|}}{Si}}-H$$

in which a bridging oxygen atom is represented by Θ.
K_1 and K_2 are the reaction rate constants and $K_e = K_1/K_2$ the equilibrium constant.

It was possible to demonstrate the formation of the reaction products $\equiv SiOH$ and $\equiv SiH$ most directly with the aid of Raman spectroscopy (Part V). The SiH vibration (2254 cm^{-1}) especially proves to be strongly Raman active, in contrast to the infrared activity of this vibration. In general Raman techniques are not the most suitable methods for making quantitative measurements. Infrared-absorption measurements are more suitable for this purpose. Because OH groups generate an absorption band at 3685 cm^{-1}, the IR-spectroscopy is the best way of determining hydroxyl concentrations in vitreous silica samples.

The absolute OH concentration is given by the formula

$$x_{\mathrm{OH}} = \frac{\beta_{\mathrm{OH}}\, M_{\mathrm{SiO_2}}}{\varepsilon_{\mathrm{OH}}\, \varrho_{\mathrm{glass}} \,.\, 100}, \tag{2}$$

where x_{OH} = mole fraction OH,
$M_{\mathrm{SiO_2}}$ = 60·1 g/mole,
$\varepsilon_{\mathrm{OH}}$ = 58 litre mole^{-1} cm^{-1},
ϱ_{glass} = 2·2 g/cm^3,
β_{OH} = optical density per mm (mm^{-1}).

$\varepsilon_{\mathrm{OH}}$ was determined in the way described in part II. Hydrogen was extracted from the samples by heating them at 1000 °C. The decrease in the β_{OH} value proved to be linearly proportional to the amount of hydrogen extracted and a value of 58 litre/mole cm was found for $\varepsilon_{\mathrm{OH}}$.

The equilibrium constant (K_e) of the reaction:

$$2\,\mathrm{SiO_2} + \mathrm{H_2} \overset{K_e}{\rightleftarrows} \equiv\mathrm{SiOH} + \equiv\mathrm{SiH} \tag{3}$$

could be determined by the formula

$$K_e = \frac{x_{\mathrm{OH}}\, x_{\mathrm{SiH}}}{x_{\mathrm{SiO_2}}{}^2\, P_{\mathrm{H_2}}} \tag{4}$$

and with $x_{\mathrm{OH}} = x_{\mathrm{SiH}} \ll 1$ and $x_{\mathrm{SiO_2}} \approx 1$, equation (4) reduces to

$$K_e \approx \frac{x_{\mathrm{OH}}{}^2}{P_{\mathrm{H_2}}}. \tag{5}$$

The validity of this relationship was checked by determining the equilibrium OH concentration for various hydrogen partial pressures at a temperature of 1550 °C (Part III). The following relationship was found

$$x_{\mathrm{OH}} = 2{\cdot}17 \,.\, 10^{-4} \sqrt{P_{\mathrm{H_2}}} \quad (\text{at } 1550\ {}^\circ\mathrm{C}). \tag{6}$$

The standard Gibbs free energy change for the reaction can be calculated directly from the relationship

$$\Delta G^0 = -RT \ln K_e.$$

The temperature dependence of ΔG^0 was studied by determining K_e at various temperatures (Part III). It was found that

$$\Delta G^0{}_{(1500-1800\ \mathrm{K})} = 34500 + 14{\cdot}25\, T\,(\mathrm{cal}). \tag{7}$$

With the aid of the temperature dependence of K_e it was possible to explain bubble formation and growth observed when cooling a melt slowly (Part I). It also made it possible to explain why at 1000 °C almost immeasurably small amounts of OH groups were retained in the samples even when they were heated in pure hydrogen.

The H_2–SiO_2 system also proved to be appropriate for studying the reaction kinetics of a solid-state/gas reaction. The reaction

$$\underset{\text{diss.}}{\equiv\text{SiOH}} + \underset{\text{diss.}}{\equiv\text{SiH}} \xrightarrow{K_2} \underset{\text{glass}}{2\,\text{SiO}_2} + \underset{\text{gas}}{\text{H}_2} \tag{8}$$

was assumed to be a second order reaction:

$$-\frac{\mathrm{d}\,x_{\mathrm{OH}}}{\mathrm{d}t} = K_2\, x_{\mathrm{OH}}{}^2. \tag{9}$$

The validity of eq. (9) could be demonstrated by determining the OH-concentration decay during heating in vacuum. In the temperature range between 600 and 800 °C the rate of H_2 evolution proved to be independent of the thickness of the samples and no OH-concentration profiles could be detected in partly extracted samples. Both these facts also indicate that the rate-determining step for hydrogen evolution is determined by reaction kinetics (Part IV). The temperature dependence of K_2 proved to be as follows:

$$K_{2\ (600-800\ ^\circ\mathrm{C})} = f \exp\left[-(63800\ \mathrm{cal}/RT)\right]. \tag{10}$$

The frequency factor f seemed to be slightly dependent on the method of preparing the vitreous-silica samples. For f a value of about $10^{12}\ \mathrm{s}^{-1}$ was found. The activation energy (63800 cal) is of the same order of magnitude as bond-breaking energies for Si–O. From the relationship $K_e = K_1/K_2$, K_1 was calculated directly.

$$K_1 = f' \exp\left(\frac{-63800}{RT}\right) . \exp\left(\frac{-34500 - 14{\cdot}25\,T}{RT}\right) \tag{12}$$

$$K_1 = f'' \exp\left(\frac{-98300}{RT}\right) \tag{13}$$

The activation energy corresponds to the energy required to break an H–H bond.

At temperatures higher than 800 °C, H_2 evolution can no longer be described by simple second-order reaction kinetics. At temperatures between 800 and 1150 °C there seems to be a competition between the rate of production of hydrogen and the retarding effect of out-diffusion of hydrogen. In this case the mathematical description of the OH decay (H_2 evolution) is very complicated. At temperatures higher than 1150 °C the rate of production of H_2 proved to be high enough for the OH-concentration decay to be described by a diffusion model. The model describing the out-diffusion of H_2 is based on the assumption that physically dissolved hydrogen is the main diffusing species and the assumption that chemical equilibrium exists locally in the sample (reaction (3)).

According to the model the OH-concentration decay can be described with the formulae as derived in paper IV.

The experimental results agree well with this model. The model predicts a *decrease* in the rate of hydrogen evolution with *increasing* temperature, a phenomenon which was found experimentally (Part IV).

Other phenomena which could be related to the reactions between H_2 and SiO_2 were also studied:

The reaction between water and vitreous silica:

$$2\,SiO_2 + H_2O \rightarrow 2\equiv SiOH \qquad (14)$$

forms hydroxyl groups that are identical with respect to the OH groups that are formed according to reaction (1). The fact that the OH groups that are formed according to reaction (14) are not compensated for with an equimolar amount of SiH groups explains why these OH groups behave more stably than OH groups that are compensated for with SiH groups.

By melting samples in wetted H_2/He atmospheres, "stable" OH groups were introduced into the samples. In this way indirect proof of the existence of SiH centres was also found (Part III).

Physically dissolved hydrogen was able to be detected in the samples by extracting them at 450 °C. Hydrogen evolution obeys the laws of normal diffusion (Part II). The presence of physically dissolved hydrogen could also be demonstrated with Raman techniques. A scattering peak at 4135 cm^{-1} was asigned to the H–H stretching vibration (Part V).

Alkali and earth-alkaline metal ion additions mask the presence of hydrogen in the glass. The intensity of the 3685 cm^{-1} absorption band decreased strongly when for example a small amount of BaO (0·1 mole %) was added. Extraction experiments showed, however, that the total amount of H_2 that was present in the doped sample scarcely differed from the total amount that was present in a freshly melted undoped sample. From the results of the extraction experiments it could be concluded that hydrogen is present not only in the form of "normal" OH and SiH groups, but also in another, chemically bonded form. (Part II).

SAMENVATTING

De chronologische volgorde waarin de diverse onderzoekingen plaatsvonden is min of meer dezelfde als de volgorde waarin de artikelen gepubliceerd zijn, die deze onderzoekingen beschrijven. Naarmate er meer gegevens beschikbaar kwamen konden betere modellen van de onderzochte verschijnselen gedefinieerd worden. In deze samenvatting zal min of meer de omgekeerde weg gevolgd worden. Eerst zullen de modellen geponeerd worden waarna met behulp van experimentele resultaten hun geldigheid wordt bewezen.

Reakties tussen waterstof en kwartsglas

Waterstof reageert met kwartsglas volgens een mechanisme waarvan het netto resultaat als volgt zal zijn:

$$\underset{\text{glas}}{2\,SiO_2} + \underset{\text{gas}}{H_2} \underset{K_2}{\overset{K_1}{\rightleftarrows}} \equiv SiOH + \equiv SiH \qquad (1)$$

waar met SiOH bedoeld wordt $SiO_{1.5}OH$ of 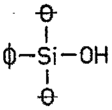

$$\phi-\overset{\theta}{\underset{\theta}{Si}}-OH$$

en met SiH bedoeld wordt $SiO_{1.5}H$ of 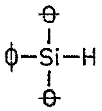

$$\phi-\overset{\theta}{\underset{\theta}{Si}}-H$$

hierin wordt een brugzuurstof voorgesteld door θ.
K_1 en K_2 zijn de reaktiesnelheidsconstanten en $K_e = K_1/K_2$ de evenwichtsconstante.

De vorming van de reaktieprodukten $\equiv$SiOH en $\equiv$SiH kon het meest direct worden aangetoond met Raman spectroscopische methoden (Deel V). Vooral de Si–H vibratie (2254 cm^{-4}) blijkt sterk Raman aktief te zijn, terwijl deze vibratie nauwelijks infrarood aktief is. In het algemeen lenen Raman-technieken zich niet al te best voor het doen van kwantitatieve metingen. Gezien het feit dat OH-groepen een IR-absorptieband doen ontstaan bij 3685 cm^{-1}, is de IR-spectroscopische methode de meest geschikte methode om hydroxylconcentraties in kwartsglazen te bepalen. De absolute OH-concentratie wordt gegeven door de formule

$$x_{\mathrm{OH}} = \frac{\beta_{\mathrm{OH}}\, M_{\mathrm{SiO_2}}}{\varepsilon_{\mathrm{OH}}\, \varrho_{\mathrm{glas}} \,.\, 100}, \tag{2}$$

waar x_{OH} = mol fractie OH,
$M_{\mathrm{SiO_2}}$ = 60·1 gr/mol,
$\varepsilon_{\mathrm{OH}}$ = 58 liter/mol cm,
ϱ_{glass} = 2·2 gr/cm^3,
β_{OH} = optische dichtheid per mm. (mm^{-1})

$\varepsilon_{\mathrm{OH}}$ werd bepaald op de wijze zoals beschreven in deel II. Waterstof werd uit de preparaten geëxtraheerd door ze te verhitten op 1000 °C. De afname van de β_{OH}-waarde bleek recht evenredig te zijn met de geëxtraheerde hoeveelheid waterstof en aldus werd een waarde van 58 liter/mol cm gevonden voor $\varepsilon_{\mathrm{OH}}$.

De evenwichtsconstanten (K_e) van de reaktie

$$2\,\mathrm{SiO_2} + \mathrm{H_2} \overset{K_e}{\rightleftarrows} \equiv\!\mathrm{SiOH} + \equiv\!\mathrm{SiH} \tag{3}$$

kon nu als volgt bepaald worden:

$$K_e = \frac{x_{\mathrm{OH}}\, x_{\mathrm{SiH}}}{x_{\mathrm{SiO_2}}{}^2\, P_{\mathrm{H_2}}} \tag{4}$$

en met $x_{\mathrm{OH}} = x_{\mathrm{SiH}} \ll 1$ en $x_{\mathrm{SiO_2}} \approx 1$ kan vergelijking (4) worden vereenvoudigd tot

$$K_e \approx \frac{x_{\mathrm{OH}}{}^2}{P_{\mathrm{H_2}}}. \tag{5}$$

De geldigheid van deze relatie werd gecontroleerd door de evenwichts-OH-concentratie bij verschillende waterstofpartiaalspanningen bij een temperatuur van 1550 °C (Deel III). De volgende relatie werd gevonden

$$x_{\mathrm{OH}} = 2{\cdot}17 \,.\, 10^{-4} \sqrt{P_{\mathrm{H_2}}} \quad \text{(bij 1550 °C)}. \tag{6}$$

De standaard Gibbs vrije energieverandering voor de reaktie kan rechtstreeks berekend worden uit de relatie:

$$\Delta G^0 = -RT \ln K_e. \tag{7}$$

De temperatuurafhankelijkheid van ΔG^0 werd bestudeerd door K_e te bepalen bij verschillende temperaturen (Deel III). Gevonden werd dat

$$\Delta G^0{}_{(1500-1800\ \mathrm{K})} = 34500 + 14{\cdot}25\, T\ \text{(cal)}. \tag{8}$$

M.b.v. de temperatuurafhankelijkheid van K_e kon de bellenvorming en -groei, die was waargenomen tijdens het langzaam afkoelen van een smelt, worden verklaard. Ook het feit dat bij 1000 °C nagenoeg onmeetbare kleine hoeveelheden OH-groepen in het glas achterbleven, zelfs wanneer de preparaten werden uitgestookt in pure waterstof, kon met deze gegevens verklaard worden.

Het systeem SiO_2–H_2 bleek ook geschikt te zijn om de reaktie kinetiek van een gas/vaste-stof reaktie te bestuderen.

$$\underset{\text{opgel.}}{\equiv\text{SiOH}} + \underset{\text{opgel.}}{\equiv\text{SiH}} \xrightarrow{K_2} \underset{\text{glas}}{2\,\text{SiO}_2} + \underset{\text{gas}}{\text{H}_2} \tag{9}$$

is een tweede orde reaktie met

$$\frac{\mathrm{d}\,X_{\mathrm{OH}}}{\mathrm{d}t} = K_2\, x_{\mathrm{OH}}{}^2. \tag{10}$$

De geldigheid van vergelijking (10) kon worden aangetoond door de OH-concentratie-afname te bepalen tijdens het verwarmen van preparaten in vacuum. In het temperatuurtraject tussen 600 en 800 °C bleek de snelheid van de waterstofafgifte onafhankelijk te zijn van de dikte van de preparaten en ook konden er geen OH-concentratieprofielen aangetoond worden in de deels geëxtraheerde preparaten. Dit zijn ook twee indicaties dat de snelheidsbepalende stap voor de waterstofafgifte bepaald wordt door de reaktiekinetiek (Deel IV). De temperatuurafhankelijkheid van K_2 is als volgt:

$$K_{2(600-800\ {}^\circ\mathrm{C})} = f \exp\,[-(63800\ \mathrm{cal}/RT)]. \tag{11}$$

De frequentiefaktor f bleek afhankelijk te zijn van de bereidingswijze van het glas. Voor f werd een waarde van ongeveer $10^{12}\ \mathrm{s}^{-1}$ gevonden. De aktiveringsenergie (63800 cal) is van dezelfde orde van grootte dan de energie die nodig is voor het breken van een SiO-binding. Uit de relatie $K_e = K_1/K_2$ werd K_1 rechtstreeks berekend.

$$K_1 = f' \exp\left(\frac{-63800}{RT}\right) \cdot \exp\left(\frac{-34500 - 14{\cdot}25\ T}{RT}\right) \tag{12}$$

$$K_1 = f'' \exp\left(\frac{-98300}{RT}\right) \tag{13}$$

De aktiveringsenergie (98300 cal) is in overeenstemming met de energie die nodig is om een mol H–H-bindingen te breken.

Bij temperaturen hoger dan 800 °C kan de waterstofafgifte niet meer worden beschreven m.b.v. eenvoudige reaktiekinetiek. In het temperatuurgebied tussen 800 en 1150 °C blijkt er concurentie te bestaan tussen de snelheid van H_2- vorming en het vertragende effekt van de „weg”diffusie H_2. In dit geval is de mathematische beschrijving van de snelheid van de OH-concentratieafname uitermate gecompliceerd. Bij temperaturen hoger dan 1150 °C blijkt de snelheid van de waterstofvorming dusdanig hoog te zijn, dat de hydroxyl-concentratieafname beschreven moet worden met een diffusiemechanisme. Het mechanisme dat de diffusie van waterstof uit het preparaat beschrijft is gebaseerd op de veronderstelling dat de fysisch opgeloste waterstof het diffunderende molecuul is en op de veronderstelling dat er plaatselijk in het preparaat chemisch evenwicht heerst (reaktie (3)). De OH-concentratieafname kan beschreven worden met de formules afgeleid in artikel IV. Het model voorspelt een *afname* van de snelheid van de waterstof afgifte bij *verhoging* van de temperatuur, een verschijnsel wat experimenteel werd gevonden (Deel IV).

Enkele andere verschijnselen welke in verband gebracht konden worden met de reakties tussen H_2 en SiO_2 werden ook bestudeerd. Bij de reaktie tussen water en kwartsglas

$$2\,SiO_2 + H_2O \rightarrow 2\equiv SiOH \qquad (14)$$

worden hydroxylgroepen gevormd die identiek zijn aan de hydroxylgroepen die worden gevormd volgens reaktie (1). Het feit dat de OH-groepen die worden gevormd volgens reaktie (14) niet worden gecompenseerd door een equimolaire hoeveelheid SiH-groepen verklaart waarom deze OH-groepen zich stabieler gedragen dan de OH-groepen die wel gecompenseerd worden door SiH-groepen. Door preparaten te smelten in een bevochtigde H_2/He atmosfeer worden "stabiele" OH-groepen in het glas geïntroduceerd. Op deze wijze kon er ook een indirect bewijs voor het bestaan van SiH-centra gevonden worden (Deel III).

Fysisch opgeloste waterstof kon worden aangetoond door de preparaten te extraheren bij 450 °C. De waterstofafgifte gehoorzaamt de wetten van de normale diffusie (Deel II). De aanwezigheid van fysisch opgeloste waterstof kon ook worden aangetoond met Raman-technieken. Een verstrooiingspiek bij 4135 cm^{-1} kon worden toegeschreven aan de H–H-stretchingvibratie (Deel V).

Alkali en aardalkali-metaalionen maskeren de aanwezigheid van waterstof in het glas. De intensiteit van de 3685-cm^{-1} absorptieband nam sterk af als b.v. een kleine hoeveelheid BaO (0,1 mol %) aan het glas werd toegevoegd. Extractie experimenten lieten echter zien dat de totale hoeveelheid waterstof die aanwezig was in de gedoteerde preparaten, nauwelijks verschilde van de totale hoeveelheid waterstof in de ongedoteerde preparaten. Uit de resultaten van de extractie-experimenten kon worden geconcludeerd dat waterstof niet alleen aanwezig is in de vorm van "normale" OH- en SiH-groepen, maar ook in een andere chemisch gebonden modificatie (artikel II).

PART I. INFLUENCE OF THE MELTING CONDITIONS ON THE HYDROXYL CONTENT IN VITREOUS SILICA

Abstract

Bubble-free vitreous silica was obtained by melting crystalline SiO_2 powder at atmospheric pressure in an H_2 (H_2/He) atmosphere at 1950 °C. The hydrogen dissolves with hydroxyl groups being formed according to the reaction

$$\underset{\text{liq.}}{3\,SiO_2} + \underset{\text{gas}}{H_2} \rightleftarrows \underset{\text{diss.}}{2\equiv SiOH} + \underset{\text{diss.}}{SiO}.$$

When the temperature is lowered the equilibrium shifts to the left which may give rise to bubble formation. Reactions between H_2O and vitreous silica result in physically identical hydroxyl groups according to the reaction

$$\underset{\text{liq.}}{2\,SiO_2} + \underset{\text{gas}}{H_2O} \rightleftarrows \underset{\text{diss.}}{2\equiv SiOH}.$$

At the melting temperature (1950 °C) an equilibrium between the hydroxyl concentration in the glass melt and the hydrogen partial pressure of the surrounding gases is not reached because of a reaction on the glass surface: $SiO_2 + H_2 \rightarrow SiO\uparrow + H_2O\uparrow$. The hydroxyl concentration in vitreous silica is determined by
(a) the H_2 partial pressure of the surrounding gas during melting;
(b) the H_2O partial pressure of the surrounding gas during melting;
(c) the sintering properties of the raw material;
(d) the thermal history of the glass;
(e) the water content of the raw material.

1. Introduction

Previous investigations have shown that it is possible to introduce water and hydrogen into vitreous silica in the form of hydroxyl groups, by treating the glass with water-containing or hydrogen-containing gases at elevated temperatures [1-6]). These reactions appear to be mainly diffusion-controlled with two different diffusion coefficients.

In the earlier investigations use was made mainly of commercially available vitreous silica, in which the hydroxyl concentration may vary from practically zero to approx. 0·1 weight%. These differences in hydroxyl content must be ascribed to differences in:

(1) production processes (H_2 and H_2O partial pressures),
(2) the raw materials used,
(3) finishing processes.

This investigation was initiated to study the influence of these factors. For this purpose a method was developed for melting crystalline SiO_2 under controlled conditions.

2. Experimental

2.1. *Equipment*

The equipment, as shown in fig. 1, has been developed to melt crystalline SiO_2 to vitreous silica under controlled conditions. The required melting temperatures were obtained by high-frequency heating of the molybdenum crucible. For reasons of temperature homogenization radiation shields were found to be necessary. The temperatures were measured by means of an optical pyrometer. Small holes (diam. 2 mm) were made in the radiation shields, so that the optical

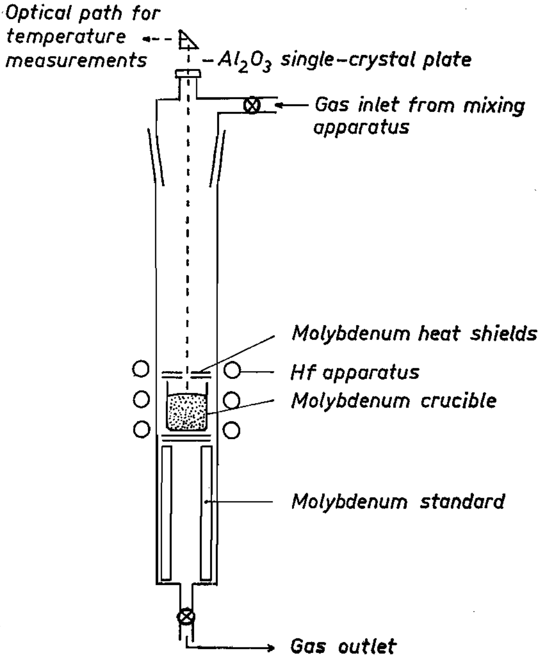

Fig. 1. Apparatus for melting vitreous-silica specimens.

path was interrupted by only a window of crystalline aluminium oxide and a vitreous-silica prism. We are aware that it is very difficult to determine the absolute temperature in this way; however, in the event it was possible to stabilize the temperature within 10 °C. The melting-equipment is connected to an installation with facilities for controlling the composition of the gas mixtures.

Small quartz crystals are melted in various gas mixtures at a pressure of one atmosphere. The controlled composition of the gas mixture is essential for obtaining a bubble-free vitreous silica within reasonable time. Melting quartz crystals enclose the surrounding atmosphere and form a bubble. The velocity at which a bubble rises is a function of the viscosity:

$$\tfrac{4}{3}\,\pi\, r^3\, \varDelta\varrho\, g = 6\,\pi\,\eta\, r\, v,$$

where v = velocity (cm/s),
$\varDelta\varrho$ = density of the glass minus the density of the gas (2·2 g/cm^3),
g = acceleration due to gravity (cm/s^2),
η = viscosity (poises),
r = radius of the bubble (cm).

In the temperature range where the melting processes occur (from 1800 to 2000 °C) the viscosity is still very high ($\eta = 10^6$ poises), so that the rising velocity of a bubble, size 100 microns, amounts to approx. $3 \,.\, 10^{-6}$ cm/min. Consequently gases of poor diffusion and solubility (N_2, Ar, CO_2) remain in bubble for very long periods of time; H_2, He and H_2O, on the other hand, are absorbed rather quickly by the molten mass of glass. Hydrogen and water react with the molten glass and dissolve in the form of hydroxyl groups. The inert helium is physically soluble and has a relatively high diffusion coefficient.

2.2. *The melting procedures*

The empty Mo crucible after firing for 5 minutes at 1950 °C and cooling was filled with quartz powder. First the system was evacuated and then the selected gas mixture was allowed to enter slowly. This was repeated once. During heating up and melting a constant gas flow of 2 l/min was maintained. The high-frequency apparatus was switched on and switched off abruptly after the melting time had elapsed (quenching). The molybdenum crucible was then dissolved in hot concentrated aqua regia, so that a quartz-glass ingot remained; this was polished bi-laterally, leaving a slide of approx. 3 mm, which was suitable for infrared-absorption measurements.

2.3. *Specifications and pre-treatment of the raw material*

Selected Brasilian rock quartz (nominal weight 4 g) was washed for 1 hour in a diluted HCl/HF solution (5% HF, 5% HCl). After acid-free rinsing and drying, the crystals were heated up to 800 °C and then dropped into cold water.

As a result of the ensuing thermal stresses the crystals break, and are thus easier to grind in a ball mill, containing vitreous-silica marbles.

The coarse crystalline powder was washed in a hot (80 °C) 10% HCl/5% HF solution. Then acid-free rinsing and drying followed by a firing procedure (during 1 hour at 1000 °C in oxygen) took place. The particle-size distribution of the raw material obtained in this way is shown in table I.

The concentrations of the impurities were determined by neutron-activation analysis. The result for the main impurities are given in table II.

TABLE 1

Particle-size distribution of milled Brasilian-quartz crystals

size (μm)	percentage
32	99·9
45	99·6
63	98·7
100	82·5
160	37·3
200	22·6
315	8·4
400	3·6
635	1·3
1000	0·5

TABLE II

Main impurities in the raw material (SiO_2) in parts per billion

Fe	100
K	80
Na	590
Ge	1100
Li	7000 *)
Al	3000 *)

*) Atomic absorption spec.

2.4. *IR-transmission measurements*

The intensity of the absorption band at 2·73 microns was determined by means of a Unicam Sp 700 A Spectrophotometer. The absorption peak for unassociated OH vibration occurs at about 2·75 μm in most hydroxylic compounds.

The β_{OH} value is defined as the optical density per mm, and is a measure of the relative hydroxyl concentrations in the samples. The absolute hydroxyl concentration can be calculated via the relation

$$[\mathrm{OH}] = \frac{\beta_{\mathrm{OH}}}{\varepsilon_v} \, \frac{M_{\mathrm{OH}} \cdot 10}{\varrho_{\mathrm{gl}}} ,$$

where $[\mathrm{OH}]$ = hydroxyl concentration (g/g glass),
β_{OH} = optical density per mm (mm^{-1}),
ε_v = molar extinction coefficient ($\mathrm{l\ mole}^{-1}\ \mathrm{cm}^{-1}$),
M_{OH} = molecular weight of hydroxyl group ($\mathrm{g\ mole}^{-1}$),
ϱ_{gl} = density of the glass ($\mathrm{g\ l}^{-1}$).

3. Results

3.1. *High-temperature reactions between hydrogen and molten* SiO_2

As postulated above, a nearly bubble-free vitreous silica can be obtained by melting small quartz crystals in an H_2/He atmosphere. This method can also be used to study the influence of the H_2 partial pressure on the hydroxyl concentration in the vitreous silica. The samples are melted in an H_2/He mixture in the way described above. The β_{OH} value as a function of the hydrogen partial pressure is presented in fig. 2. In our opinion the increase of hydroxyl groups is possibly a result of the following reduction reaction:

$$\underset{\text{liq.}}{3\,\mathrm{SiO_2}} + \underset{\text{gas}}{\mathrm{H_2}} \rightleftarrows \underset{\text{dissolved}}{2\,\equiv\!\mathrm{SiOH}} + \underset{\text{dissolved}}{\mathrm{SiO}} \, . \tag{1}$$

The hydroxyl groups and possibly also the silicon monoxide are incorporated in the glass structure.

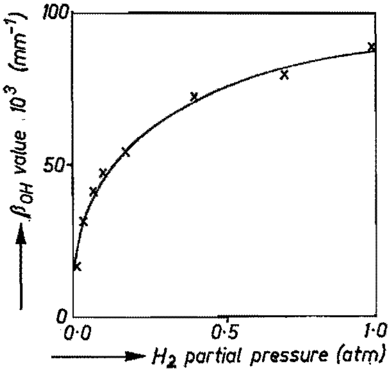

Fig. 2. Variation of the β_{OH} value for specimens melted at different hydrogen pressures.

Bell, Hetherington and Jack [2,9]) propose a different reaction mechanism, according to which trivalent silicon atoms are formed. According to this mechanism the samples should contain considerable quantities of paramagnetic Si^{3+} ions. Up till now, however, we have not succeeded in detecting this paramagnetic ions by means of ESR measurements.

Various tests have indicated that at the melting temperatures no equilibrium is reached between the reaction products in the vitreous silica and the surrounding gases. This is shown by the following experiments.

Experiment I

A sample was melted in a 99% He/1% H_2 atmosphere at 1950 °C. After 15 minutes this flow was replaced by a H_2 flow for 60 minutes. No perceptible increase in the β_{OH} value was established.

During the 75 minutes the experiment lasted, a large part of the quartz glass had reacted. This phenomenon gave rise to a trial series, the evaporation rate being determined as a function of the hydrogen partial pressure (see fig. 3).

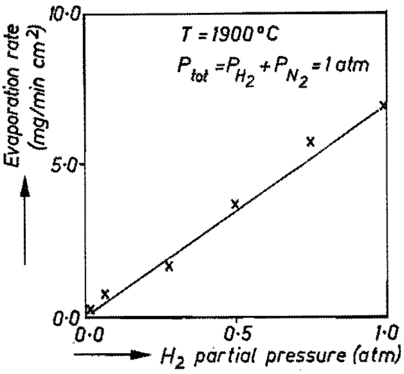

Fig. 3. Evaporation rate of vitreous silica in mg/min cm² as a function of the hydrogen partial pressure.

The temperature dependence of the evaporation rate is shown in fig. 4. The conclusion may be drawn that the penetration of the hydrogen into the molten glass mass is probably prevented by a reaction occurring on the molten-glass surface, whereby the volatile reaction products are drained with the gas flow:

$$SiO_2 + H_2 \rightarrow SiO\uparrow + H_2O\uparrow. \qquad (2)$$

This reduction reaction has been studied by several investigators [10-13]). It is likely that a similar reaction takes place on the surface of an included gas bubble. In this case, however, the reaction products cannot be drained, but will dissolve in the quartz glass:

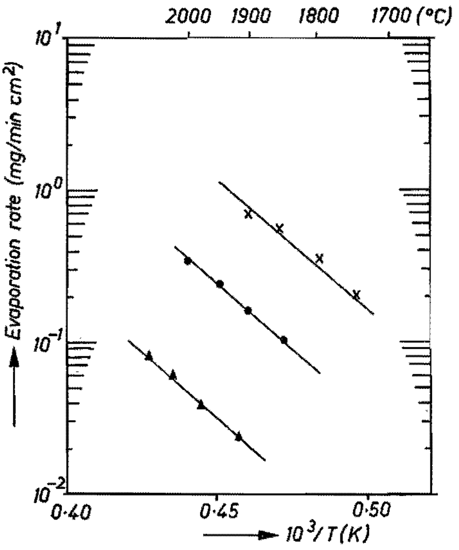

Fig. 4. Temperature dependence of the evaporation rate of vitreous silica at different hydrogen pressures; × hydrogen : nitrogen = 1 : 0,
● hydrogen : nitrogen = 27 : 73,
▲ hydrogen : nitrogen = 0 : 1.

$$\underset{}{2\,SiO_2} + \underset{gas}{SiO} + \underset{gas}{H_2O} \leftrightarrows \underset{diss.}{2 \equiv SiOH} + \underset{diss.}{SiO}\,. \qquad (3)$$

The nett result of the two consecutive reactions (2) and (3) is the same as that of reaction (1).

Experiment II

A sample was melted in a 100% H_2 atmosphere (15 minutes at 1950 °C). In this case the H_2 flow was replaced by an He flow (60 minutes at 1950 °C). The β_{OH} value in the quartz glass did not perceptibly decrease in this procedure. Presumably the diffusion of hydrogen in vitreous silica follows a mechanism in which the physically dissolved hydrogen molecules (and not the hydroxyl groups) play an essential part [13]).

The concentration of the physically dissolved H_2 is determined by the equilibrium constant K of reaction (1). As during melting in an H_2 atmosphere no H_2 is supplied to the bulk (experiment I), a local equilibrium is reached in the bulk between the physically dissolved and the chemically bonded hydrogen. There are two indications that the concentration of the physically dissolved H_2 will be lower than the saturation concentration at 1 atmosphere, viz.

(a) During melting in an H_2 atmosphere the bubbles filled with hydrogen disappear completely. This shows that at this temperature the vitreous silica is not yet saturated with H_2.

(b) Results to be published later [8]) have shown that in the temperature range between 1200 and 1500 °C an equilibrium can be reached between the surrounding atmosphere and the hydrogen in the quartz glass. In this temperature range the evaporation rate of the quartz glass has become small with respect to the diffusion rate of the H_2. When these data are extrapolated to 1950 °C, the calculated β_{OH} value will be considerably higher than the experimentally found value.

When the concentration of physically dissolved H_2 in the vitreous silica is small, its transport by diffusion will also be small; consequently the hydroxyl concentration during the experiment (60 minutes) will hardly decrease.

The results of the above-mentioned experiments lead to the conclusion that in an early stage of the melting process a quantity of hydrogen is included, which will hardly change during the melting process. This would mean that the sintering properties and thus the particle-size distribution of the raw material must play an important role. At a certain stage of the sintering process (which precedes melting) a quantity of hydrogen is entrapped between the grains. In general, sintering properties are strongly influenced by the particle-size distribution of the raw material. To investigate this, the raw material was split up into five sieving fractions. These samples were melted in an H_2/He mixture. The effect on the β_{OH} value of the glass samples is demonstrated in table III.

TABLE III

Influence of particle-size distribution on the β_{OH} value of vitreous silica, after melting in a 50%H_2–50%He mixture

particle size (μm) of the quartz powder	β_{OH} value of vitreous silica
300–600	$71{\cdot}7 \,.\, 10^{-3}$
200–300	$68{\cdot}7 \,.\, 10^{-3}$
160–200	$62{\cdot}0 \,.\, 10^{-3}$
100–160	$55{\cdot}2 \,.\, 10^{-3}$
63–100	$36{\cdot}6 \,.\, 10^{-3}$
table-I distribution	$76{\cdot}0 \,.\, 10^{-3}$

In view of this model, however, a linear dependence between the H_2 partial pressure and the β_{OH} value could be expected. For the rather strong deviation which is found between the expected linear dependence and the experimental results (fig. 2), in our opinion, the following possible explanation can be given:

(a) The sintering properties of the crystalline material are also determined by the sintering atmosphere.

(b) The raw material itself is a hydrogen source (though a constant one); see further sec. 3.4.

(c) Within the finite quenching period of the sample, the reverse reaction can partly proceed while physically dissolved hydrogen is formed. This H_2 is not detected with the IR-transmission measurement.

3.2. *Hydrogen development and bubble formation during cooling*

On account of the temperature dependence of the equilibrium constant the equilibrium state of reaction (1) will be influenced during the cooling process.

The equilibrium strongly shifts to the left, which appears from tests in which quartz glasses with a high β_{OH} value were fired under H_2 atmosphere at 1000 °C for 24 hours. The β_{OH} values of samples thus treated were decimated. A typical example is the following.

A sample was melted in an H_2 atmosphere at 1950 °C for 15 minutes. By cooling down the melt to 1700 °C, maintaining it at this temperature for 5 minutes and then quenching it, a bubble-rich quartz glass is obtained (fig. 5).

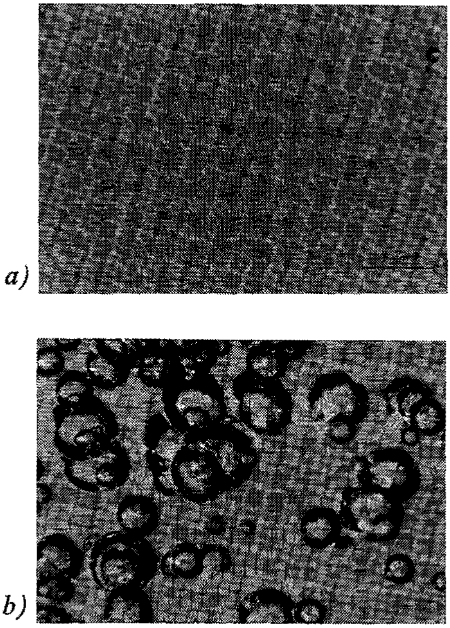

Fig. 5. Bubble pattern of a rapidly and a slowly cooled vitreous-silica sample. Melting conditions: temperature: 1950 °C, time: 15 minutes, pressure: 1 atm H_2.
(*a*) Melting procedure followed by rapid cooling.
(*b*) Melting procedure followed by heating for 15 minutes at 1700 °C and rapid cooling.

A micro breaking device, included in the circuit of a gas chromatograph, was used to determine the hydrogen pressure in bubbles of different diameter (cf.

table IV). A shift of equilibrium during cooling causes physically dissolved hydrogen to be formed. According to Henry's law,

$$P = c\,[H_2] \text{ (physically dissolved)},$$

when the hydrogen concentration becomes large, the corresponding pressure will exceed atmospheric pressure and a tendency towards bubble formation will arise.

Generally bubble growth in a liquid is described with two coupled differential equations [14]:
an ordinary differential equation

$$R\frac{\mathrm{d}^2R}{\mathrm{d}t^2} + \tfrac{3}{2}\left(\frac{\mathrm{d}R}{\mathrm{d}t}\right)^2 + \frac{4\eta}{R\varrho}\left(\frac{\mathrm{d}R}{\mathrm{d}t}\right) + \frac{2\sigma}{R\varrho} = \frac{\Delta P}{\varrho} \tag{4}$$

and the partial differential equation

$$\frac{\partial c}{\partial t} + \frac{R^2}{r^2}\,\frac{\mathrm{d}R}{\mathrm{d}t}\,\frac{\partial c}{\partial r} = D\left(\frac{\partial^2 c}{\partial r^2} + \frac{2}{r}\,\frac{\partial c}{\partial r}\right), \tag{5}$$

where R = bubble radius,
η = viscosity,
σ = surface tension,
ϱ = density of the melt,
ΔP = pressure differences (inside and outside the bubble),
c = hydrogen concentration,
r = distance from the centre of the bubble.

TABLE IV
Hydrogen pressure in bubbles of different sizes. The bubbles are grown at 1700 °C at 1 atm H_2 pressure for 15 minutes

bubble diameter (μm)	H_2 pressure (atm) in the bubble at 1700 °C (calculated from room-temperature pressure in the bubble)
960	1·98
790	1·92
580	1·98
415	4·36
330	4·10
240	6·60
187	9·50

In our case eq. (4) can be simplified to the extent of neglecting the first two inertia factors. This approximation is justified because of the fact that the viscosity of the liquid is very high (appr. 10^8 poises) and the bubble diameter is very small (10–100 μm). Equation (4) then changes into

$$\frac{4\,\eta}{R}\left(\frac{\mathrm{d}R}{\mathrm{d}t}\right)+\frac{2\sigma}{R}=\Delta P \tag{6}$$

with the following solution:

$$\frac{R(t)}{R_0}=\frac{2\sigma}{R_0\,\Delta P}\left(1-\exp\frac{\Delta P\,t}{4\eta}\right)+\exp\frac{\Delta P\,t}{4\eta}. \tag{7}$$

Table V gives the maximum size (calculated according to eq. (7)) which a bubble with an initial diameter of 10 microns can assume. The initial diameter of 10 microns has been chosen because a quenched sample contains a small number of bubbles with a main diameter of 10 microns which will probably act as a nucleus. Comparison of the experimental values from table IV with the calculated values from table V warrants the conclusion that diffusion equation (5) plays an important role in bubble-growth kinetics. To solve the mathematical problem accurately would be very complicated because of some unknown factors.

TABLE V

Maximum bubble radius, calculated according to eq. (7), with: $R_0 = 5 \,.\, 10^{-4}$ cm, $t = 900$ s, $\sigma = 400$ dynes/cm, $\eta = 10^8$ poises, and ΔP is assumed to be constant during growing

ΔP (atm)	R_{900} (μm)	remarks
1·0	—	bubble should have shrunk
1·63	5·0	no bubble growth
2·0	$9{\cdot}4 \,.\, 10$	
3·0	$2{\cdot}0 \,.\, 10^3$	
10·0	$4{\cdot}1 \,.\, 10^{10}$	

3.3. *High-temperature reactions between water and vitreous silica*

Water was introduced into the system by wetting the applied H_2/He mixtures. With the existing equipment a maximum dew point of 25 °C can be reached. In this trial series the H_2/He series ratio was kept constant (23 : 77) and the water partial pressure was varied between 0 and about 0·03 atm.

The glass samples prepared in this way were fired in a vacuum atmosphere for several hours at 1000 °C. The hydroxyl content as a function of firing time of a sample treated in H_2/He and in H_2/H_2O/He is given in fig. 6. The con-

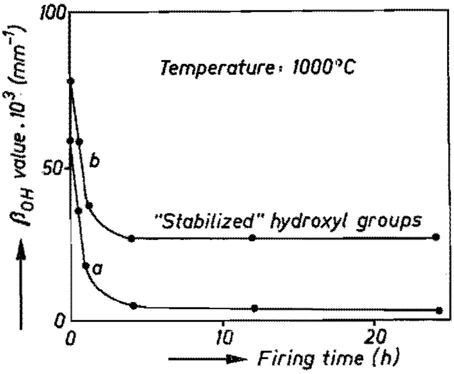

Fig. 6. β_{OH} value of vitreous-silica samples prepared by ourselves and fired in vacuum at 1000 °C.
a: Thickness of the sample: 1·5 mm, melted in a dry 77 %He/23 %H_2 mixture.
b: Thickness of the sample: 1·5 mm, melted in a wettened (dew point 22 °C) 77 %He/23 %H_2 mixture.

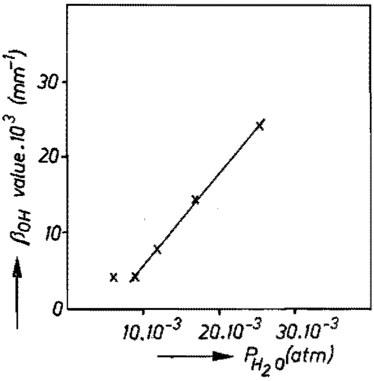

Fig. 7. β_{OH} value of vitreous-silica samples melted at different water-vapour pressures, after firing for 24 h (1000 °C) in vacuum. The hydrogen–helium ratio was kept constant during melting (23 : 77).

centration of the remaining ("stabilized") hydroxyl groups proves to be dependent on the applied water-vapour pressure (cf. fig. 7). Probably the following reaction will take place:

$$\underset{\text{liq.}}{2\,SiO_2} + \underset{\text{gas}}{H_2O} \rightleftarrows \underset{\text{diss.}}{2 \equiv SiOH}. \tag{8}$$

The essential difference between the reactions (1) and (8) is that with reaction (1) not only are hydroxyl groups formed, but also a reduced centre. This reduced centre is oxidized at 1000 °C by the decomposing hydroxyl groups, while hydrogen is formed.

The hydroxyl groups originating from the type-(8) reactions are not compensated for by an equivalent number of reduced centres, and as a higher-valency situation of the silicon and/or a peroxide formation are highly improbable, physically dissolved water will inevitably be formed during dissociation of the hydroxyl groups. As known from literature ²) the diffusion coefficient for water at 1000 °C is about a factor 1000 smaller than the same coefficient for hydrogen. Probably this is the reason why the OH groups originating from a reaction with molecular water are more difficult to remove from the quartz glass. Experiments in which H_2 and H_2O in the surrounding gases were replaced by D_2 and/or D_2O, respectively, have shown that type-(1) and type-(8) hydroxyl groups are completely interchangeable.

3.4. *The raw material as hydroxyl source*

When the crystalline quartz powder is melted in an evacuated hydroxyl-free vitreous-silica ampulla, in an arrangement which bears much resemblance to the arrangement as shown in fig. 1, a bubble-free quartz glass is formed with a β_{OH} value of $20 \,.\, 10^{-3}$ mm^{-1}. These hydroxyl groups apparently belong to the category which is hard to remove (reaction (8)). After 24 hours of firing at 1000 °C in vacuum the β_{OH} value has hardly changed ($\beta_{OH} = 19 \,.\, 10^{-3}$ mm^{-1})

As during the melting process H_2 and H_2O were excluded from the system, the hydroxyl groups must originate from the raw material. This was confirmed by using various raw materials, as a result of which the β_{OH} value varied between $10 \,.\, 10^{-3}$ and $70 \,.\, 10^{-3}$ mm^{-1}. This gives rise to the question why the glasses that were prepared in a dry H_2/He atmosphere contain no (or hardly any) "stabilized" hydroxyl groups. A probable explanation is the following.

As long as the quartz crystals have not yet been completely sintered or melted a certain product of the already initiated reduction reaction can be drained relatively more quickly via the pores:

$$\underset{\text{sol.}}{SiO_2} + \underset{\text{gas}}{H_2} \rightarrow \underset{\text{gas}}{H_2O} + \underset{\text{sol.}}{SiO}$$

↓

partly disappears via the pores (e.g. as a result of a temperature increase),

partly stays behind the pores and later dissolves in the form of hydroxyl groups.

Almost the entire SiO formed may stay behind in the bulk, e.g. as a condensate or included in the network.

According to this mechanism

$$[\text{oxidator } (= OH)] < [\text{reductor } (= Si^{2+})].$$

The hydroxyl groups carried along by the raw material can now (partly) compensate for the shortage of oxidant. This model also explains the phenomenon that the formation of "stabilized" hydroxyl groups (as a result of adding water to the gas) becomes perceptible only with $P_{H_2} > 10^{-2}$ atm (fig. 7).

3.5. *Behaviour of the helium during the melting process*

When the He partial pressure was increased to above 0·5 atm, the melting times required to obtain a bubble-free quartz glass became increasingly longer. Under such conditions the vitreous silica is probably saturated with He. This finding gave rise to the trend of the bubble pattern being studied as a function of the melting time. Figure 8 shows the quartz-glass samples that were melted in a 99% He atmosphere. Attention is drawn to the fact that after some time

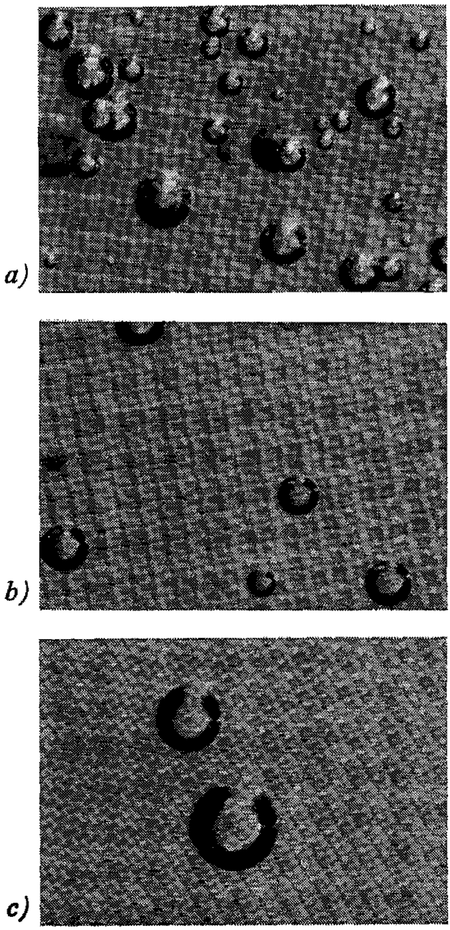

Fig. 8. Bubble patterns of vitreous-silica samples. Melting conditions: temperature: 1950 °C, gas mixture: 99%He/1%H_2 (1 atm).
(*a*) Melting time 5 minutes, rapid cooling.
(*b*) Melting time 10 minutes, rapid cooling.
(*c*) Melting time 30 minutes, rapid cooling.

the smaller bubbles disappear, while the nominal diameter of the remaining bubbles increases. Finally also the larger bubbles disappear.

The surface tension is the driving force for these shrinking and growing processes:

$$\Delta P = \frac{2\sigma}{R}.$$

The gas in the small bubbles will have a higher absolute pressure than the gas in the large bubbles. The concentration of the physically dissolved helium around the bubbles adapts to the He pressure in the bubble (according to Henry's law). These concentration gradients make gas transport possible. As the mutual distances between the bubbles are much smaller, on the average, than the distance between a bubble and the melting surface (or crucible wall), first of all there will be a mutual exchange of gas between the bubbles, as a result of which the smaller bubbles dissolve and the larger ones grow. At a later stage the larger bubbles also dissolve due to gas transport to surface and crucible wall. This process, however, is perceptibly slower on account of the relatively long diffusion paths and small pressure gradients.

4. Conclusions

(a) Important factors contributing to the hydroxyl content of vitreous silica are:

(1) the hydrogen and water partial pressures of the surrounding gas during melting;
(2) the particle-size distribution of the raw material;
(3) the hydroxyl content of the raw material;
(4) the heat treatment after melting.

(b) There are probably two reasons why equilibrium between the melt and the surrounding hydrogen- and water-containing atmosphere is not reached:

(1) A reaction at the glass surface $SiO_2 + H_2 \rightarrow SiO\uparrow + H_2O\uparrow$ prevents the penetration of hydrogen into the molten glass mass. The removal rate of the reaction products was found to be linearly proportional to the hydrogen partial pressure.
(2) The removal of hydrogen out of the melt is a very slow process, the concentration of physically dissolved hydrogen being very low; therefore mass transport by diffusion is bound to be very small.

(c) Because of the temperature dependence of the equilibrium constant K of the reaction

$$3\,SiO_2 + H_2 \rightleftarrows 2 \underset{\text{diss.}}{\equiv SiOH} + \underset{\text{diss.}}{SiO}$$

bubbles can be formed by hydrogen development during cooling.

(d) The apparent difference in stability of hydroxyl groups at 1000 °C should perhaps be ascribed to differences in oxidation state of the glass network. As long as oxidizable centres are available, hydrogen should evolve. When, however, oxidizable centres are no longer available, water is likely to be formed. The removal rate of hydrogen and water from the vitreous silica is a function of the diffusion coefficient, the physical solubility and the geometry of the sample.

The conversion of hydroxyl groups to oxygen bonds and H_2 (or H_2O) is hampered by the rate of removal of one of the reaction products.

The rate of removal of physically dissolved water is relatively much slower than that of physically dissolved hydrogen.

5. Final remarks

(a) Recent experiments have shown that it is possible to determine the temperature dependence of the equilibrium reaction

$$\underset{\text{liq.}}{3\,\mathrm{SiO_2}} + \underset{\text{gas}}{\mathrm{H_2}} \rightleftarrows \underset{\text{diss.}}{2\,{\equiv}\mathrm{SiOH}} + \underset{\text{diss.}}{\mathrm{SiO}}$$

in the temperature range 1200 to 1550 °C.

(b) The first results of extraction experiments have shown that the hydrogen content of vitreous-silica samples does not agree with the value calculated from the 2·73-μm absorption band. Use was made of the molar extinction coefficient ($\varepsilon_v = 77{\cdot}5$ l mole^{-1} cm^{-1}), which was determined by, among others, Stephenson and Jack [7]).

(c) According to the authors, complex formation between hydroxyl groups and negatively charged centres in the glass lattice or the formation of Si–H bonds, may explain the discrepancy between the results of the extraction experiments and the results calculated from IR-absorption measurements.

REFERENCES

[1]) A. J. Moulson and J. P. Roberts, Trans. Faraday Soc. **57**, 1208, 1961.
[2]) T. Bell, G. Hetherington and K. H. Jack, Phys. Chem. Glasses **3**, 141, 1962.
[3]) S. P. Faile and D. M. Roy, J. Amer. ceram. Soc. **54**, 533, 1971.
[4]) J. F. Shackelford, University of California, UCRL - 20399, 1971.
[5]) G. J. Roberts and J. P. Roberts, Phys. Chem. Glasses **5**, 79, 1964.
[6]) T. Drury and J. P. Roberts, Phys. Chem. Glasses **4**, 79, 1963.
[7]) G. W. Stephenson and K. H. Jack, Trans. Brit. ceram. Soc. **59**, 397, 1960.
[8]) G. H. A. M. van der Steen and E. Papanikolau, Philips Res. Repts **30**, 309, 1975 (Part III of this thesis).
[9]) G. Hetherington and K. H. Jack, Phys. Chem. Glasses **5**, 147, 1964.
[10]) K. Schwerdtfeger, Trans. metallurgical Soc. AIME **236**, 1152, 1966.
[11]) R. A. Gardner, J. solid State Chem. **9**, 336, 1974.
[12]) H. F. Ramstadt, F. D. Richardson and P. J. Bowles, Trans. metallurgical Soc. AIME **221**, 1021, 1961.

13) N. C. Tombs and A. J. E. Welch, J. Iron and Steel Inst. **172**, 62, 1952.
14) R. W. Lee, J. chem. Phys. **38**, 448, 1963.
15) E. J. Barlow and W. E. Langlois, IBM J. Res. Dev. **6**, 329, 1962.

PART II. CHEMICAL AND PHYSICAL SOLUBILITY OF HYDROGEN IN VITREOUS SILICA

Abstract

Hydrogen dissolves in vitreous silica at elevated temperatures accompanied by the formation of $\equiv$Si–OH groups and an equimolar amount of other H-containing centres. Below 600 °C the kinetics of the reverse reaction is very slow and the hydroxyl concentration does not decrease during heat treatment. Physically dissolved hydrogen is easily removable at 450 °C, and the evolution of hydrogen obeys the laws of normal diffusion. Above 600 °C, the evolution of hydrogen is linearly proportional to the decrease of the OH concentration. Small amounts of alkali and alkaline-earth-metal ions may considerably influence the chemically bonded state of the hydrogen present in the vitreous silica.

1. Introduction

In general the concentration of hydroxyl groups in vitreous silica can be estimated by making use of the extinction coefficient (ε_{OH}) and assuming the validity of the Beer–Lambert law:

$$[OH] = \frac{10\,\beta_{OH}\,M_{OH}}{\varepsilon_{OH}\,\varrho_{gl}}\ \text{g OH/g of glass},$$

where $[OH]$ = hydroxyl concentration (g OH/g of glass),
β_{OH} = optical density per mm (mm^{-1}),
M_{OH} = molecular weight of a hydroxyl group (g mole^{-1}),
ε_{OH} = practical extinction coefficient (litre mole^{-1} cm^{-1}),
ϱ_{gl} = density of the glass (g litre^{-1}).

In general the absorption band of the unassociated hydroxyl vibration occurs at about 3700 cm^{-1}.

Stephenson and Jack [1]) determined ε_{OH} by studying the weight lost by a Spectrosil sample during firing in vacuo at 1000 °C. The loss in weight, assumed to be water, was related to the optical density. Two experiments gave respectively 78 and 77 l mole^{-1} cm^{-1} for ε_{OH}. In the literature the extinction coefficient for water or for hydroxyl groups is used more or less arbitrarily. To avoid confusion, the authors will indicate in the course of the paper whether the extinction coefficient refers to –OH groups (ε_{OH}) or to water (ε_{H_2O}). Hydroxyl groups can be introduced in vitreous silica by melting the quartz powder in a hydrogen-containing atmosphere. This has been shown in a previous publication [2]). It is shown there also that the state of oxidation of the underlying glass network determines whether H_2 or H_2O is evolved during heating in vacuo. Because of the relatively high diffusion coefficient of hydrogen in vitreous silica, it is quickly removed from the glass sample as the reaction proceeds. The removal of H_2O from the glass is a slow process compared with H_2 evolution, probably due to the small diffusivity of water in vitreous silica. At high temperatures (> 1500 °C) hydrogen formation, due to decomposing OH groups may even give rise to bubble formation.

The construction of an extraction apparatus suitable for determining very small amounts of hydrogen makes it possible to study the relation between the $\Delta\beta_{OH}$ value and the hydrogen concentration and thus to determine the "practical" molar extinction coefficient of hydroxyl in vitreous silica. In this paper it is also demonstrated that small amounts of alkali and alkaline-earth metals have a great influence on the chemical behaviour of hydrogen in the glass.

2. Preparation of the vitreous-silica samples

2.1. *Melting procedure*

The raw material (rinsed and milled Brazilian rock quartz) was melted in a molybdenum crucible in a hydrogen atmosphere at 1950 °C by a high-frequency technique. A more detailed description of the melting apparatus, raw material and melting procedures has been given in a previous publication [2]). The vitreous-silica ingots were polished bilaterally, so that a thin plate, suitable for absorption and extraction measurements, remained.

2.2. *Barium addition*

Barium was added to the crystalline quartz powder in the form of a solution of its nitrate. In order to spread the solution as homogeneously as possible over the quartz powder and also to prevent the formation of concentration gradients during drying, such an amount of solution was added that the surface of the crystals was wetted but no pools were formed (about 0·5 cm^3 solution/g of quartz). After drying at 200 °C, the mixture was stirred in an agate mortar and fired for one hour at 1050 °C in an oxygen atmosphere. The mixture was melted in the same way as an undoped sample.

The Ba content (after melting) was determined with the aid of atomic-absorption analysis.

2.3. *Equipment for high-temperature treatments*

Some samples were fired in a vertical high-temperature tube furnace (PCA 10/10 (1800 °C) Lab. Furnace) at temperatures between 1100 and 1600 °C in an H_2/N_2 atmosphere.

The samples were quenched in the same atmosphere as they were heated in. The glass plates were placed in a molybdenum crucible and the temperature was measured by means of a pyrometer. Samples with varying hydroxyl content can be produced by varying the partial pressure of the hydrogen and/or changing the heating temperature.

After the heat treatment the surface of the vitreous-silica plates had generally recrystallized. After repolishing, the IR-absorption measurement and extraction experiment took place.

3. Apparatus for extraction experiments

The extraction experiments took place in an apparatus as described schematically in fig. 1. After IR-absorption measurement the glass plate was treated with a concentrated HF solution, rinsed with distilled water, and dried at 50 °C. This treatment was necessary in order to remove surface contaminants. After drying, the sample was placed in a vitreous-silica tube A which was sealed to the system.

The sample could be moved in the system by means of two magnets B1 and B2. The magnet inside the system was mounted in a small evacuated vitreous-silica capsule. Prior to the start of the experiment, the sample was pushed into the cold zone of tube A, oven C was heated up (1000 °C), and the system was evacuated by means of a mercury-diffusion pump D until a pressure of 10^{-7} Torr was reached. Valve E was then turned off. The very slow decay of the high-vacuum meter indicated that leakage from the system was very small. The oven was now cooled down and the sample pushed to the centre of the oven. The temperature was raised again and the extraction experiment started. By means of a Toeppler pump, F, the gases were concentrated in volume G. A float in volume G prevented the concentrated gases as well as a small amount of mercury from flowing back into the Toeppler pump. The pump concentrated the gas at a speed of about two strokes a minute. Concentrating the gases was performed automatically by detection of the mercury level in tube H with a light source and a photoconductivity cell. During every stroke about 50% of the gases present in the system was transported to volume G. During the last stroke the mercury level was raised to the top of capillary I. Accordingly the gas was forced into a channel drilled in valve J. By turning this valve, the channel was connected with the circuit of a gas chromatograph.

The gas chromatograph was provided with a column about 7 metres in length, filled with molecular sieves 13 X (30–50 meshes). The column temperature was kept constant at 50 °C, while the carrier gas (Ar) flowed at a speed of 30 ml/min. At the end of the column a catharometer (type Gow–Mac 10–285 WX) was mounted. The detection limit for the system described above was 10^{-7} cm^3 (N.T.P.) H_2.

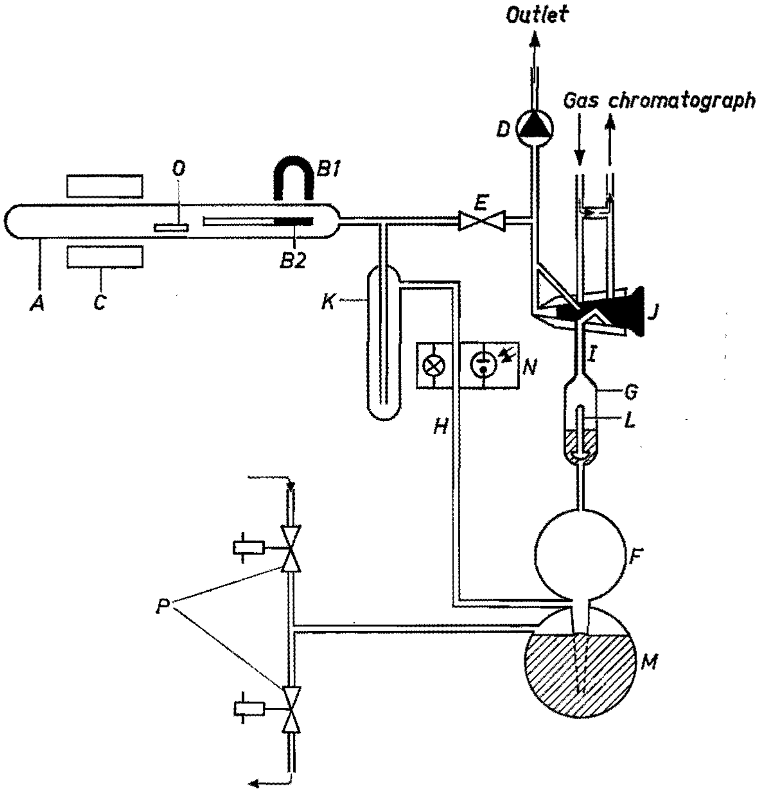

Fig. 1. Apparatus for extraction experiment.

A = vitreous-silica tube,
B1, B2 = magnets,
C = oven,
D = mercury-diffusion pump,
E = valve,
F = Toeppler pump,
G = glass capsule provided with a float (L),
H = glass tube
I = capillary,
J = valve, with a channel drilled in it. This valve can occupy 3 positions:
1. to evacuate the channel,
2. to fill the channel with the extracted gas,
3. to connect the channel with the circuit of the gas chromatograph,
K = N_2-cooled trap
L = float,
M = mercury,
N = light source and photoconductivity cell (connected with P),
O = sample,
P = magnetic stopcocks connected with N.

To operate the apparatus in practice, more valves and high-vacuum meters are connected to the system.

4. Equipment for absorption measurements

The infrared-absorption measurements were carried out with a Jasco IRA-2 spectrophotometer (4000–400 cm^{-1}). For measurements in the near-ultraviolet and visible-light regions (50000–4000 cm^{-1}) a Beckmann DK-2 was used. Difference spectra were recorded by placing one of the samples in the reference beam of the spectrophotometer.

5. Results and discussion

5.1. *IR-absorption measurements*

Faile and Roy [3]) introduced large amounts of OH groups into vitreous silica by means of neutron irradiation in a hydrogen-containing atmosphere. Their experiments indicated that when the OH concentration in the sample is very great, the absorption spectrum is extended by two bands (2250 and 4520 cm^{-1}). The first band was attributed to the fundamental Si–H stretching vibration and the other to its first overtone.

It is known from "Silane" chemistry that the fundamental Si–H stretching vibration occurs as a rule at frequencies between 2300 and 2100 cm^{-1}, with corresponding overtones at between 4600 and 4200 cm^{-1}. Si–H bonds are also presumed to occur in silicon-device technology, where thin SiO_2 layers are grown at the silicon surface by thermal or anodical oxidation [4]).

In our preparation technique it is equally possible that Si–H bonds are formed:

$$2\,SiO_2 + H_2 \rightarrow {\equiv}Si\text{–}H + {\equiv}Si\text{–}OH, \qquad (1)$$

where

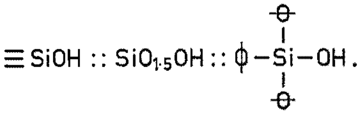

$$\equiv SiOH :: SiO_{1.5}OH :: \phi-\overset{\theta}{\underset{\theta}{Si}}-OH.$$

The OH concentration in our glass, however, is some orders of magnitude lower than the concentration in the irradiated glasses that were produced by Faile and Roy. For accurate measurements it is necessary to have samples with a relatively high Si–H concentration or very thick samples. The preparation of thick, bubble-free samples is hampered by the fact that quenching becomes less effective and bubbles, filled with hydrogen, are formed during cooling.

We succeeded in preparing a thick, practically bubble-free sample by melting the quartz powder in a 25% H_2–75% He mixture. After cutting and polishing, a plate of about 14·4 mm thickness remained. One of the two halves of the plate was fired for 60 hours at 1050 °C in vacuo.

Figure 2 gives the absorption spectra of both samples as well as the difference spectrum.

An absorption band of a low intensity was recorded at 4535 cm^{-1} (untreated sample). Unfortunately, vitreous silica itself has some very strong absorption bands in the 2200-cm^{-1} region. This probably explains why we were unable to record an absorption band at 2250 cm^{-1}.

We have not yet been able to decide whether the 4535-cm^{-1} absorption band should be attributed to an Si–H vibration or to a vibration of an asymmetric tetrahedron containing a hydroxyl group (as proposed by Adams [5])), or to both.

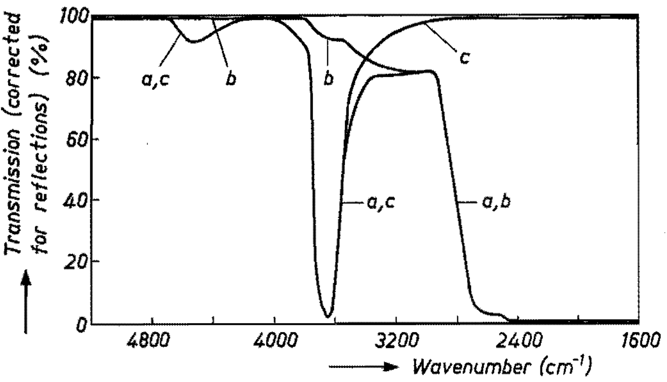

Fig. 2. Absorption spectra of (a): vitreous silica melted in a 25% H_2–75% He atmosphere; (b) sample (a) fired for 60 h at 1050 °C in vacuum; (c) difference spectrum ((a) — (b)). Thickness of the samples 14·4 mm.

5.2. *Separation of physically dissolved and chemically bonded hydrogen by means of extraction*

The effect of temperature treatment on the β_{OH} value of a freshly melted sample can be described as follows. When a freshly melted vitreous-silica sample with a β_{OH} value of $70 \,.\, 10^{-3}$ mm^{-1} was fired for 1000 hours in vacuo at 450 °C, the β_{OH} value did not decrease detectably during this treatment. When the sample was fired at 750 °C for the same period of time a slow decrease of the β_{OH} value was observed. At 1000 °C the β_{OH} value was reduced to about $1 \,.\, 10^{-3}$ mm^{-1} within a few hours.

When a similar sample was extracted in an apparatus as described in sec. 3, the results were as follows. At 450 °C the sample released $1{\cdot}97 \,.\, 10^{-2}$ cm^3 (N.T.P.) H_2/g of glass within 24 hours. After 24 hours, hydrogen evolution had stopped almost completely. When the temperature was raised to 700 °C, hydrogen development restarted slowly. At 1000 °C the evolution of hydrogen was very fast during the first hours of extraction. Between 600 and 1000 °C, $12{\cdot}8 \,.\, 10^{-2}$ cm^3 (N.T.P.) H_2/g of glass was released and the β_{OH} value went to zero.

The observed qualitative effects of firing on H_2 evolution and on the β_{OH} value are given in table I. These results confirm the assumption that at lower temperatures the chemical interaction between the glass network and the diffusing hydrogen molecules is negligibly small.

If there is no appreciable interaction between the physically dissolved H_2 and the glass network, the evolution of gas must obey the laws of normal diffusion. As a first approximation the small flat plates (thickness of the plate about 3 mm, diameter 20 mm) were taken to be a semi-infinite plane sheet. The solution of Fick's equation for this system then becomes:

TABLE I

Qualitative effect of heat treatment on hydrogen development and on the β_{OH} value of an undoped and a Ba-doped vitreous-silica sample

temperature (°C)	evolution of H_2 by		β_{OH} value	
	undoped sample	Ba-doped sample	undoped sample	Ba-doped sample
450	fast stops after 24 hours	fast stops after 24 hours	no change	no change
500	none	none	no change	no change
600	very slow	fast stops after 130 hours	very slow decrease	decreases at the same rate as H_2 development, until zero
700	slow	none	decreases at the same rate as H_2 development	remains zero
750	slow	slow	,,	remains zero
1000	fast	fast	,,	remains zero

$$\bar{c} = \frac{1}{h}\int_0^h c\,\mathrm{d}x = \frac{8c_0}{\pi^2}\sum_{n=0}^{\infty}\frac{1}{(2n+1)^2}\exp\left[-\left(\frac{(2n+1)\,\pi}{h}\right)^2 D\,t\right], \tag{2}$$

where $\bar{c}$ = mean concentration,
c_0 = initial concentration,
h = thickness of the sample,
D = diffusion coefficient,
t = time,
x = distance $(0 < x < h)$.

A more detailed treatment of this mathematical problem is given in the publications by Jost [6]) and Crank [7]).

With the aid of computer techniques the extraction data of the sample can be compared with the calculated values and the diffusion coefficient adapted

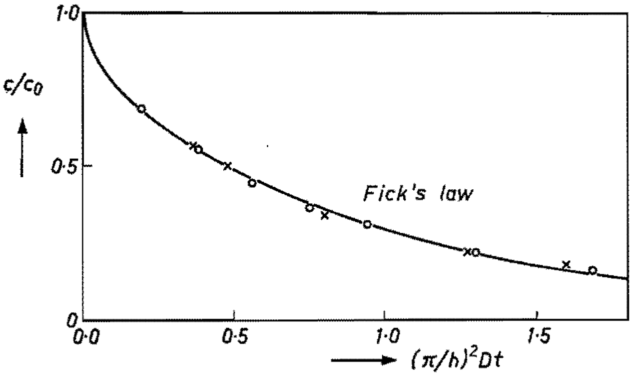

Fig. 3. Typical outdiffusion curves. Firing temperature 450 °C. × Vitreous silica, $D = 4{\cdot}37 \,.\, 10^{-7}$ cm^2 s^{-1}, $h = 0{\cdot}221$ cm. ○ Vitreous silica, 0·1 mole% BaO, $D = 3{\cdot}34 \,.\, 10^{-7}$ cm^2 s^{-1}, $h = 0{\cdot}230$ cm. Calculated Fick's-law curve (drawn) is shown for comparison.

until the theoretical curve shows an optimum fit with the experiment (cf. fig. 3). The diffusion coefficient corresponding to the best-fitting curve is $4{\cdot}37 \,.\, 10^{-7}$ cm^2 s^{-1}, a value which is quite well comparable with the results of Lee [14]) ($D_{450\,^\circ\mathrm{C}} = 4{\cdot}54 \,.\, 10^{-7}$ cm^2 s^{-1}).

Most probably the concentration of physically dissolved hydrogen in the samples is *not* equal to the saturation hydrogen concentration at 1 atmosphere. During the finite cooling time, hydrogen will be formed as a result of decomposing hydroxyl groups. As shown in an earlier publication [2]), slow cooling may even give rise to bubble formation. The pressure in these bubbles may exceed the atmospheric pressure considerably (up to 10 atmospheres in a bubble with a diameter of about 200 μm).

A sample with a different thermal history was prepared as follows. A freshly melted sample was reheated for 16 hours at 1550 °C in a hydrogen atmosphere and quenched. As a result of this treatment the β_{OH} value was reduced to $43 \,.\, 10^{-3}$ mm^{-1}.

When this sample was extracted at 450 °C, $0{\cdot}71 \,.\, 10^{-2}$ cm^3 (N.T.P.) H_2 per g of glass was evolved.

In our opinion these experiments indicate that the concentration of physically dissolved hydrogen is strongly dependent on the thermal history of the samples.

5.3. *The practical molar extinction coefficient for* OH *groups in vitreous silica*

When the physically dissolved hydrogen is removed from the samples at 450 °C, the chemically bonded modification will still be present. Samples of a series having different β_{OH} values were extracted at temperatures between 600 and 1000 °C and the results are given in fig. 4. The straight line indicates that $\varepsilon_{\mathrm{OH}}$ is independent of the concentration.

In order to calculate the molar extinction coefficient for OH *groups* from

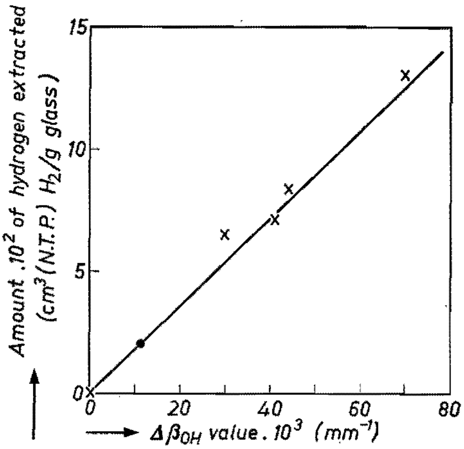

Fig. 4. Extracted amounts of chemically bonded hydrogen (in the form of Si–OH and Si–H groups) as a function of the β_{OH} value. Before plotting, the amount of physically dissolved hydrogen (extracted at 450 °C) is subtracted from the total amount. Point • refers to a Ba-doped sample, extracted at 600 °C.

this figure, some additional information is necessary, for it is important whether one H_2 molecule produces one or two hydroxyl groups. For instance

$$Si^{4+}\,2\,O^{2-} + \tfrac{1}{2}\,H_2 \rightarrow \underbrace{Si^{3+}O^{2-}OH}_{\text{reduced silica with hydroxyl}} \quad \text{(suggested by Bell}^{8)}\text{)} \qquad (3)$$

or ²)

$$3\,SiO_2 + H_2 \rightarrow \underbrace{2\,{\equiv}SiOH + SiO}_{\text{dissolved}} \qquad (4)$$

are two reaction mechanisms where one H_2 molecule produces two OH groups.

Another possibility is the following mechanism:

$$\equiv Si\text{–}O\text{–}Si\equiv + H_2 \rightarrow \equiv SiOH + H\text{–}Si\equiv, \qquad (5)$$

where one H_2 molecule forms one OH group and one Si–H group. Assuming that the OH groups are formed according to reaction (3) or (4), the extinction coefficient will come to $\varepsilon_{OH} = 29{\cdot}0$ l mole⁻¹ cm⁻¹, whereas, if the OH groups are formed according to reaction (5) the extinction coefficient will be twice as high, $\varepsilon_{OH} = 58{\cdot}0$ l mole⁻¹ cm⁻¹. The latter value is not too far from the extinction coefficient determined by Stephenson ¹) $\varepsilon_{OH} = 77{\cdot}5$ l mole⁻¹ cm⁻¹. In the authors' opinion there exists a strong indication that equimolar amounts of Si–OH- and Si–H-type groups are formed by reaction (5). Assuming that this reaction mechanism is valid, some phenomena can easily be explained, viz.:

(a) The relationship

$$K P_{H_2} = [\equiv SiOH]\,[\equiv SiH] = [OH]^2.$$

is consistent with the experimental results ⁹).

(b) In silicon-device technology thin vitreous-silica films can be grown on silicon plates by for example thermal oxidation. Beckmann [4]) measured the infrared-absorption spectra of these films by internal-reflection spectroscopy and attributed absorption bands at 2250 and 2350 cm^{-1} to the fundamental Si–H . . O and to Si–H stretching vibration respectively.

(c) The shape of the etchant count profiles for SiO_2 films formed by thermal oxidation with titrated water [10]) have been explained by Breed [11]), making use of this reaction mechanism.

(d) The results of recent H–D-exchange experiments support the assumption that considerable amounts of hydrogen must be present in the glass in a form other than hydroxyl groups [9]).

In our previous paper [2]) it was assumed that the reaction products formed within a bubble by the reaction

$$SiO_2 + \underset{\text{gas}}{H_2} \rightarrow \underset{\text{gas}}{SiO} + \underset{\text{gas}}{H_2O}$$

were dissolved in the network according to

$$2\,SiO_2 + \underset{\text{gas}}{SiO} + \underset{\text{gas}}{H_2O} \rightarrow 2 \underset{\text{diss.}}{\equiv SiOH} + \underset{\text{diss.}}{SiO};$$

if this process is followed by some rearranging reaction:

$$2 \underset{\text{diss.}}{\equiv SiOH} + \underset{\text{diss.}}{SiO} \rightarrow \underset{\text{diss.}}{\equiv SiOH} + \underset{\text{diss.}}{\equiv SiH} + SiO_2\,,$$

the net result will be the same as for the reaction (5).

Another possibility is the formation of a strong complex between one hydroxyl group and the Si^{2+}-containing centre:

$$\underbrace{\equiv SiOH\ SiO} + \equiv SiOH.$$

It is known that strong complex hydrogen bridges can shift the absorption bands to lower frequencies. If the complex is strong, the absorption band may even shift to frequencies where the glass itself has some very strong absorption bands. As a consequence of this, only half of the OH groups would be visible at 3700 cm^{-1}. The difference between an Si–H group and a strong complex may be a gradual one. Because of the low dielectric constant of the glass (as compared with water), complex formation is quite possible even at high temperature.

5.4. *Vitreous silica with* BaO *dopes*

Scholze [12]) and Götz [13]) studied the influence of the addition of glass modifiers in soda-lime-silicate glasses on the behaviour of the OH absorption bands in the 3300-cm^{-1} region. To study the influence of modifiers on the behaviour of H_2 in vitreous silica, we prepared samples in the manner described in sec. 2.2. Experiments showed that the effect of the addition of alkali and alkaline-earth-metal ions was roughly the same. We chose Ba-doped samples for a more extensive study, because Ba addition seemed to be fairly well reproducible (low evaporation loss). The β_{OH} value of the Ba-doped samples seems to be strongly dependent on the Ba concentration. In fig. 5 the β_{OH} value is given as a function of the Ba concentration.

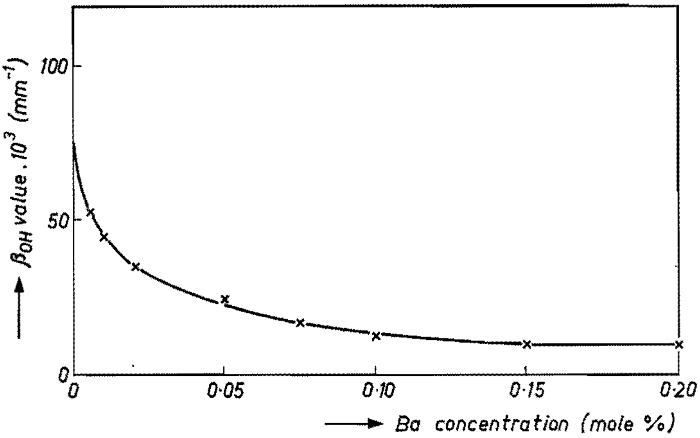

Fig. 5. β_{OH} value as a function of the Ba concentration in vitreous-silica samples. The samples were melted for 15 min at 1950 °C in a hydrogen atmosphere.

In the case of low Ba concentrations the effect on the β_{OH} value is particularly striking. Except for the absorption bands due to–OH and Si–H vibrations, the spectrum of a doped sample looks similar to the spectrum of an undoped sample. The difference spectrum of a doped and an undoped sample does not show any additional absorption bands either. The extraction data, however, differ markedly from the data for undoped samples.

When a freshly melted sample containing 0·1 mole% BaO was extracted at 450 °C, $1{\cdot}38 \cdot 10^{-2}$ cm^3 (N.T.P.) H_2/g of glass was evolved. This amount is comparable with the amount that is released from undoped samples. The diffusion coefficient is slightly lower than the diffusion coefficient of H_2 in an undoped sample ($D_{450\,°C} = 3{\cdot}34 \cdot 10^{-7}$ $cm^2\,s^{-1}$ and $D_{450\,°C} = 4{\cdot}37 \cdot 10^{-7}$ $cm^2\,s^{-1}$, respectively) (cf. fig. 3).

A second experiment, carried out with a sample of about half the thickness, gave the same result. In contrast with the undoped samples, H_2 development starts again at 600 °C, while the β_{OH} value decreases simultaneously ($\Delta\beta_{OH} = 12 \cdot 10^{-3}$ mm^{-1}, $2{\cdot}18 \cdot 10^{-2}$ cm^3 (N.T.P.) H_2/g of glass). This amount of H_2 evolved at 600 °C seems to be quite well predictable with the aid of the curve in fig. 4 (the experimental point has been added in that figure).

When the sample is "empty" with respect to physically dissolved H_2 and –OH groups, H_2 development stops. When, however, the temperature is raised to 1000 °C, H_2 development starts again ($5{\cdot}85 \,.\, 10^{-2}$ cm^3 (N.T.P.) H_2/g of glass).

This leads to the conclusion that there must be some other hydrogen-containing centre, rather than the normal –OH and Si–H groups in the glass, which cannot be visualized with the normal IR-absorption techniques. In 0·1-mole%-doped samples most of the hydrogen is in fact present in this unknown chemically bonded state (table II). The qualitative effects of heat treatment on the hydrogen development and the β_{OH} value are given in table I.

TABLE II

Extraction data for a 0·1-mole% BaO-doped vitreous-silica sample

temperature (°C)	amount of H_2 extracted in cm^3 (N.T.P.)/g of glass	remarks
450	$1{\cdot}38 \,.\, 10^{-2}$	β_{OH} value remains $12 \,.\, 10^{-3}$ mm^{-1}
600	$2{\cdot}18 \,.\, 10^{-2}$	β_{OH} value decreases until zero
700–1000	$5{\cdot}85 \,.\, 10^{-2}$	β_{OH} value remains zero

6. Discussion and conclusions

(1) Physically dissolved hydrogen can be removed separately from the chemically bonded hydrogen by firing the vitreous silica at 450 °C in vacuo.

(2) Hydrogen development at 450 °C obeys the laws of normal diffusion with $D_{450\,^{\circ}C} = 4{\cdot}37 \,.\, 10^{-7}$ cm^2 s^{-1}.

(3) The amount of physically dissolved hydrogen present in a sample is strongly dependent on the thermal history of the sample. During cooling (or quenching) an unknown amount of OH groups and Si–H groups will decompose and form H_2.

It may be possible to study the solubility as well as the diffusivity of H_2 in vitreous silica at temperatures below 550 °C by making use of the extraction technique described. Above 550 °C the data are clouded by a chemical interaction between the diffusing H_2 molecules and the SiO_2 network.

(4) When a sample, which is "empty" with respect to physically dissolved H_2, is heated up to 600 °C, H_2 development restarts very slowly, while the

β_{OH} value decreases simultaneously. In the temperature range between 750 and 1000 °C, H_2 development is very fast, and the β_{OH} value decreases at the same rate. This leads to the conclusion that decomposing –OH (and Si–H) groups act as H_2 sources. A value of 58 $\mathrm{l\,mole^{-1}\,cm^{-1}}$ is found for ε_{OH}.

(5) In BaO-doped samples three types of hydrogen can be distinguished.

(a) Physically dissolved hydrogen, which leaves the sample at 450 °C, obeying the laws of normal diffusion with $D_{450\,°C} = 3{\cdot}34 \,.\, 10^{-7}\ \mathrm{cm^2\,s^{-1}}$. The diffusion coefficient is somewhat lower than the diffusion coefficient of H_2 in an undoped sample.

(b) Chemically bonded H_2 in the form of Si–OH and Si–H groups. The extinction coefficient for OH groups is the same as the extinction coefficient for OH groups in undoped samples. The thermal stability of the OH and Si–H groups is affected by BaO addition.

(c) Most of the hydrogen is bonded in a more stable form. So far it has not been possible to visualize these H_2-containing centres with the aid of normal IR-absorption measurements.

(6) The effect of BaO addition on the absorption band at 3700 $\mathrm{cm^{-1}}$ is much stronger than the effects measured by Scholze [12]) and Götz [13]) in soda-lime-silicate glasses. The formation of a new absorption band at about 2800 $\mathrm{cm^{-1}}$ could not be detected either. One of the possible ways of explaining this is to assume that strong hydrogen bridges are formed, so that the frequency for OH stretching shifts to the 1600-$\mathrm{cm^{-1}}$ range.

(7) In general, it is no use trying to calculate the total H_2 (or H_2O) content of vitreous silica with the aid of the OH concentration, measured by means of IR absorption, without knowing the other factors.

The H concentration in vitreous silica is made up of the following terms:

$$[\mathrm{H}] = 2\,x\,\frac{10\,\beta_{OH}}{\varrho_{gl}\,\varepsilon_{OH}} + (1-x)\,\frac{10\,\beta_{OH}}{\varrho_{gl}\,\varepsilon_{OH}} + [\mathrm{H}]_{\mathrm{phys.\,diss.}} + 2\,[\mathrm{H_2O}]_{\mathrm{phys.\,diss.}} +$$

$$+ [\mathrm{H}]_{\mathrm{chem.\ bonded\ other\ than\ \equiv SiOH\ and\ \equiv SiH}}$$

where x is the fraction of –OH groups that is compensated by an equal amount of Si–H groups.

(a) x can be estimated by firing the sample at 1050 °C in vacuo for 24 hours and measuring the β_{OH} value.

(b) $[\mathrm{H}]_{\mathrm{phys.\,diss.}}$ may vary considerably and is determined mainly by the thermal history during cooling. Extraction of the H_2 at 450 °C gives the most direct information about the concentration.

(c) $[\mathrm{H_2O}]_{\mathrm{phys.\,diss.}}$ is probably negligibly small.

(d) $[\mathrm{H}]_{\mathrm{chem.\ bonded,\ etc.}}$ This concentration is strongly dependent on the alkali content and may account for up to about 80% of the total hydrogen content. Hence it may in some cases be the most important H_2 source.

(8) The anomalies of the input and decay portions of the permeation data found by Lee 14,15) can probably be explained if the reduction reaction between H_2 and SiO_2 is assumed. In the temperature range in which Lee found the anomalies (> 600 °C), the amount of OH groups formed due to this reaction is too small to measure with the aid of IR-absorption techniques. The much more sensitive extraction experiments show the presence of chemically bonded hydrogen very clearly. The anomalies in the results of the H–D-exchange experiments, carried out by the same author, are probably attributable to the presence of Si–H groups that participate in the exchange reactions. The equilibrium constant for the reaction $2\,SiO_2 + H_2 \rightleftarrows \equiv SiOH + (\text{“}\equiv SiH\text{”})$ seems to be strongly temperature-dependent. We intend to publish the results of these investigations in the near future.

REFERENCES

1) G. W. Stephenson and K. H. Jack, Trans. Brit. ceram. Soc. **59**, 397, 1960.
2) G. H. A. M. van der Steen and E. Papanikolau, Philips Res. Repts **30**, 103, 1975 (Part I of this thesis).
3) S. P. Faile and R. M. Roy, Mat. Res. Bull. **5**, 385, 1970.
4) K. H. Beckmann and N. J. Harrick, J. electrochem. Soc. **118**, 614, 1971.
5) R. V. Adams, Ph. D. Thesis, University of Sheffield, 1960.
6) W. Jost, Diffusion, Methoden der Messung und Auswertung, Dr. Dietrich Steinkopff Verlag, Darmstadt.
7) J. Crank, Mathematics of diffusion, Clarendon Press, Oxford, 1957, p. 347.
8) T. Bell, G. Hetherington and K. H. Jack, Phys. Chem. Glasses **3**, no. 5, 141, 1962.
9) G. H. A. M. van der Steen, Philips Res. Repts **30**, 309, 1975 (Part III of this thesis).
10) D. J. Burkhardt, J. electrochem. Soc. **114**, 196, 1967.
11) D. J. Breed, submitted to J. elektrochem. Soc.
12) H. Scholze, Glastechn. Ber. **32**, 81, 142, 278, 314, 381, 421, 1959.
13) J. Götz and E. Vosáhlová, Glastechn. Ber. **41**, 47, 1968.
14) R. W. Lee, R. C. Frank and D. E. Swets, J. chem. Phys. **36**, 1062, 1962.
15) R. W. Lee and D. L. Fry, Phys. Chem. Glasses **7**, no. 1, 19, 1966.

PART III. SOME THERMODYNAMIC DATA ON THE REDUCTION OF VITREOUS SILICA

Abstract

On the basis of the data given in this and earlier published papers [1,2]) it can be concluded that hydrogen dissolves in vitreous silica according to a reaction of the following type:

$$2\,SiO_2 + H_2 \rightleftarrows \equiv SiOH + \equiv SiH$$

where

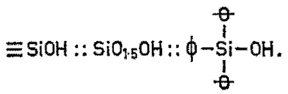

$$\equiv SiOH :: SiO_{1{\cdot}5}OH :: \phi - \overset{\overset{\theta}{|}}{\underset{\underset{\theta}{|}}{Si}} - OH.$$

with

$$\Delta G^0{}_{1500-1800\,K} = 34500 + 14{\cdot}25\,T \quad \text{(cal)}.$$

The change in Gibbs free energy seems to be slightly dependent on the glass-preparation technique. A linear relationship is found between the OH mole fraction and the square root of the hydrogen partial pressure. Bubble formation during the cooling of a melt can be explained with the aid of these thermodynamic data. The results of experiments where H_2 (D_2)/H_2O (D_2O) mixtures were used during melting, support a reaction mechanism according to which equimolar amounts of $\equiv$SiOH and $\equiv$SiH groups are formed.

1. Introduction

Some data have been published on the thermodynamics of the reduction of (vitreous) silica by hydrogen [3,4,5,7]). Most investigations on the reduction of silica concern the reaction [3,4,5])

$$\begin{array}{cccc} SiO_2 + & H_2 \rightarrow & SiO + & H_2O. \\ \text{cryst.} & \text{gas} & \text{gas} & \text{gas} \end{array} \tag{1}$$

This reaction seems to have a strongly endothermic character. According to Ramstadt [5]):

$$\Delta G^0{}_{1700-1900\,K} = 127100 - 45{\cdot}07\,T \quad \text{(cal)}.$$

Hydrogen can be introduced in the form of $\equiv$SiOH groups and $\equiv$Si–H centres [2]) according to the reaction

$$\underset{\text{glass}}{2\,\mathrm{SiO_2}} + \mathrm{H_2} \rightarrow \equiv\mathrm{SiOH} + \equiv\mathrm{SiH} \tag{2}$$

where

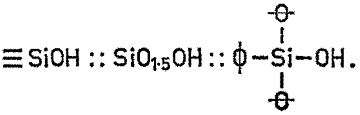

$$\equiv\mathrm{SiOH} :: \mathrm{SiO_{1.5}OH} :: \mathrm{O}{-}\overset{\displaystyle -\mathrm{O}-}{\underset{\displaystyle -\mathrm{O}-}{\mathrm{Si}}}{-}\mathrm{OH}.$$

The vitreous-silica network is considered to be the solvent for the hydrogen-containing centres. If the gaseous reaction products from reaction (1) are dissolved in the glass network, accompanied by some rearrangement reaction (or complex formation), the net result will be the same as for reaction (2). The difference between the Gibbs-free-energy changes of reactions (1) and (2) is attributable to the heat effects and entropy changes of the following reaction:

$$\underset{\text{gas}}{\mathrm{H_2O}} + \underset{\text{gas}}{\mathrm{SiO}} + \underset{\text{glass}}{\mathrm{SiO_2}} \rightarrow \equiv\mathrm{SiOH} + \equiv\mathrm{SiH}. \tag{3}$$

This work is concerned with the study of reaction (2). A phenomenon like bubble formation during the cooling of a melt can be explained with the aid of the data found.

Another reaction which introduces hydroxyl groups into vitreous silica is the reaction between water and the glass:

$$\underset{\text{glass}}{2\,\mathrm{SiO_2}} + \underset{\text{gas}}{\mathrm{H_2O}} \rightarrow 2\equiv\mathrm{SiOH}. \tag{4}$$

This reaction has been studied by Moulson and Roberts [6]). Reaction (2) combined with reaction (4) can be used to demonstrate the existence of ≡SiH-like centres.

2. Experimental

2.1. *Preparation of the samples*

Milled and rinsed Brasilian-rock crystals were melted in a molybdenum crucible at 1950 °C in an H_2/He atmosphere. A more detailed description of the raw material and melting procedures has been given in an earlier paper [1]). Plates of about 3 mm thickness were cut from the glass ingot and polished bilaterally.

At the melting temperature (1950 °C) equilibrium OH concentration is not reached. The penetration of hydrogen into the melt is probably hampered by a reaction at the surface of the melt [1]). At lower temperatures ($<$ 1550 °C) the kinetics of this reaction has become negligibly small and equilibrium conditions for reaction (2) can be reached. In order to establish equilibrium conditions, the vitreous-silica plates were fired for 16 hours in an electrically heated vertical-tube furnace (PCA 10/10 Lab furnace), at the desired temperature and hydrogen partial pressure. The hydrogen partial pressure was changed by mixing H_2 and N_2 in a mixing apparatus. The use of several accessories made it possible to quench the samples in the same atmosphere as that in which they were fired.

When the samples were heated at temperatures between 1200 and 1500 °C, the surface of the glass plates was usually recrystallized and therefore the samples had to be repolished.

The intensity of the 2·73-μm absorption band was measured with the aid of a Jasco-IRA 2 double-beam spectrophotometer.

In determining the OH mole fraction (x_{OH}) with the aid of the 2·73-μm absorption band, the practical molar extinction coefficient, which relates the optical density per mm (β_{OH} value) to the hydroxyl concentration, plays an important role. In a previously published work [2]) we have described an extraction method for determining the extinction coefficient, a value of 58 $l\,\mathrm{mole}^{-1}\,\mathrm{cm}^{-1}$ is found for ε_{OH} and therefore:

$$x_{OH} = \frac{10\,\beta_{OH}\,M_{SiO_2}}{\varepsilon_{OH}\,\varrho_{glass}}, \qquad (5)$$

where x_{OH} = mole fraction OH,
M_{SiO_2} = 60·1 g/mole,
ϱ_{glass} = 2200 g/litre,
ε_{OH} = 58 litre/mole cm,
β_{OH} = optical density per mm.

3. Results and discussion

3.1. OH *concentration in vitreous silica as a function of the* H_2 *partial pressure*

The vitreous-silica plates were fired at 1550 °C in an H_2/N_2 mixture for 16 hours and quenched. After repolishing, the β_{OH} value was measured (β_{OH} value = optical density per mm).

Real equilibrium conditions should be independent of the path followed. To check this, two types of samples were used.

Type a: Freshly molten samples (15 min, 1950 °C, 100% H_2, quenched) with a β_{OH} value higher than the equilibrium β_{OH} value.

Type b: Samples fired for 24 hours in vacuum at 1050 °C. This treatment reduces the β_{OH} value to practically zero.

Figure 1 indicates whether the initial OH concentration was higher (O) or lower (×) than the equilibrium concentration. A linear relationship is observed between the square root of hydrogen partial pressure and the OH concentration ($x_{OH} = 2{\cdot}17\,.\,10^{-4}\,\sqrt{p_{H_2}}$ at 1550 °C).

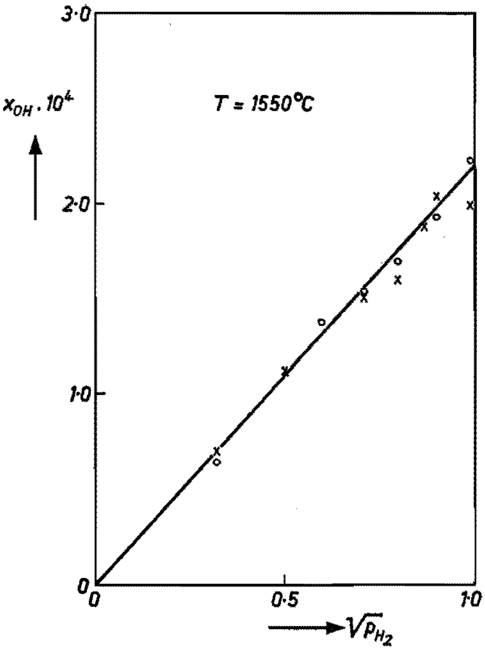

Fig. 1. Mole fraction of hydroxyl as a function of the square root of the hydrogen partial pressure. O: initial OH concentration higher than equilibrium concentration; ×: initial OH concentration lower than equilibrium concentration.

3.2. *Standard Gibbs-free-energy changes for the reduction reaction*

In studying the temperature dependence of the reaction, nearly the same procedure was followed as in studying the pressure dependence, except for the fact that in this case the hydrogen pressure was held constant (1 atmosphere) while the temperature was changed. Assuming that reaction (2) is valid, the following relationship will hold:

$$\Delta G^0 = -RT \ln K = -RT \ln \left(\frac{\gamma_{OH}\, x_{OH}\, \gamma_{SiH}\, x_{SiH}}{\gamma_{SiO_2}{}^2\; x_{SiO_2}{}^2\, f\, p_{H_2}} \right), \qquad (6)$$

where

γ_{SiO_2}, γ_{OH}, γ_{SiH} are the activity coefficients of the various reactants,

f is the fugacity coefficient for hydrogen,

x_{SiO_2}, x_{OH}, x_{SiH} are the mole fractions,

ΔG^0 is the standard Gibbs-free-energy change for reaction (2), where one mole hydrogen has reacted to ≡SiOH and ≡SiH groups in the form of a hypothetically ideal solution.

When the fugacity coefficient f is taken unity and $\gamma_{OH}, \gamma_{SiH}, \gamma_{SiO_2} = 1$ for $x_{SiOH}, x_{SiH} \to 0$, with $x_{OH} = x_{SiH}$, and x_{SiO_2} assumed to be constant, equation (6) reduces to

$$\Delta G^0 = -RT \ln \frac{x_{OH}^2}{p_{H_2}} . \tag{7}$$

In fig. 2, ΔG^0 is plotted as a function of temperature. The best-fitting straight line gives

$$\Delta G^0 = 34500 + 14{\cdot}25\,T \quad \text{(cal)} \quad \text{(glass 1).} \tag{8}$$

The reaction thus seems to be endothermic, with a negative entropy change ($\Delta G^0 = \Delta H^0 - T\,\Delta S^0$). The negative entropy change is probably mainly due to disappearance of the gaseous hydrogen.

The only known thermodynamic quantities for hydroxyl groups in vitreous silica were reported by Moulson [6]) and Bell [7]). Moulson studied the reaction between water and vitreous silica (reaction (4)) and found $\Delta H_S = -6$ kcal/mole. Bell investigated the reaction between hydrogen and vitreous silica. The heat of solution found by Bell ($\Delta H_S = -2$ kcal/mole) differs considerably from our own values and even the sign of the heat effect is different. This is prob-

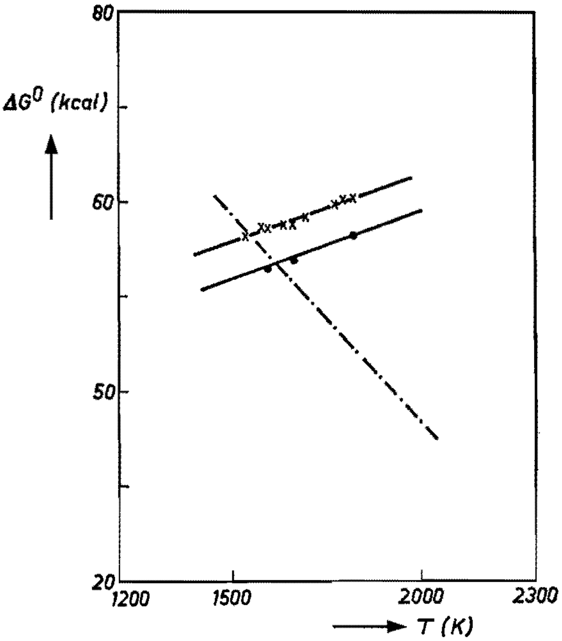

Fig. 2. Standard Gibbs-free-energy changes as a function of temperature for the reactions

(A) $\underset{\text{glass}}{2\,SiO_2} + \underset{\text{gas}}{H_2} \rightarrow \underset{\text{diss.}}{\equiv SiOH} + \underset{\text{diss.}}{\equiv SiH}$ (×: glass 1, •: glass 2),

(B) $\underset{\text{glass}}{SiO_2} + \underset{\text{gas}}{H_2} \rightarrow \underset{\text{gas}}{SiO} + \underset{\text{gas}}{H_2O}$ (dash-dotted).

(Reaction (B) according to Ramstadt [5]), corrected for the crystalline-glass transition.)

ably due to the fact that Bell derived the reaction enthalpy from only two measuring points (800 and 1050 °C). According to our experiments, the equilibrium OH concentration is very low in this temperature range and very difficult to measure accurately.

Between 1700 and 1850 K, thermodynamic data are obtained for reaction (1) ($\Delta G^0 = 127100 - 45{\cdot}07\,T$) [5]) and for reaction (2) ($\Delta G^0 = 34500 + 14{\cdot}25\,T$ (this paper)), see fig. 2.

In the study of reaction (1), crystalline SiO_2 powder was used. The thermochemical properties of the vitreous state differ slightly from those of the crystalline state. This can be compensated for as follows:

$$\begin{array}{llllll}
SiO_2 + & H_2 & \rightarrow SiO & + H_2O, & \Delta G^0 = 127100 - 45{\cdot}07\,T & \\
\text{cryst.} & \text{gas} & \text{gas} & \text{gas} & & \\
 & SiO_2 & \rightarrow SiO_2, & & \Delta G^0 \approx -2900 + 1{\cdot}20\,T & \\
 & \text{glass} & \text{cryst.} & & & \\
\hline
SiO_2 + & H_2 & \rightarrow SiO & + H_2O, & \Delta G^0 \approx 124200 - 43{\cdot}87\,T & \quad (9) \\
\text{glass} & \text{gas} & \text{gas} & \text{gas} & &
\end{array}$$

The arrangement used in studying reduction reaction (2) (firing a vitreous-silica plate in a continuous H_2 flow in an electrically heated furnace) can be considered as a closed system for this reaction. However, the system is not a closed one with respect to reaction (1). Taking this into account in conjunction with the fact that the standard Gibbs-free-energy change is less positive for reaction (1) than for reaction (2), one would expect gaseous SiO and H_2O to be formed rather than OH groups.

A consideration of the rate-controlling processes may explain why nevertheless a quasi-equilibrium OH concentration is reached. Hydrogen penetrates into vitreous silica at a rate approximately 1000 times greater than the rate at which H_2O moves within the glass. Within the plate, the hydrogen reaction will be accompanied by the formation of physically dissolved H_2O and SiO. The rate of removal of these products will be considerably slower than the rate of production. Therefore, in practice, the reactions that occur in the bulk will hardly be affected by the composition of the surrounding atmosphere (except for the H_2 partial pressure).

The formation of OH and SiH groups may therefore also be considered as a result of the next reaction:

$$\begin{array}{lllll}
SiO + & H_2O + & SiO_2 \rightarrow & \equiv SiOH + \equiv SiH & \quad (10) \\
\text{gas} & \text{gas} & \text{glass} & &
\end{array}$$

with

$$\Delta G^0 = -89700 + 58{\cdot}12\,T \quad \text{(cal)}. \qquad (11)$$

3.3. *Bubble formation when cooling a melt*

Another interesting relationship is that between log β_{OH} and the reciprocal temperature:

$$\frac{d \ln K}{d(1/T)} = \frac{d \ln x_{OH}^2}{d(1/T)} = 4{\cdot}6 \frac{d \log \beta_{OH}}{d(1/T)}. \tag{12}$$

Log β_{OH} as a function of $1/T$ is shown in fig. 3. With the aid of this figure one can explain the interesting phenomenon of bubble growth when a melt is slowly cooled.

In a previous paper ¹) it was shown that, when a sample was melted in a hydrogen atmosphere at 1950 °C and then cooled down to 1700 °C and held at this temperature for 15 minutes, a great number of hydrogen-filled bubbles was formed.

It was also shown that at 1950 °C the equilibrium OH concentration is not reached, due to a fast evaporation process at the surface of the melt. The total amount of hydrogen present in the glass is mainly determined by the amount that is included during heating, sintering and melting. A typical β_{OH} value for a freshly melted sample comes to 90 . 10^{-3} mm^{-1}. It can be seen from fig. 3,

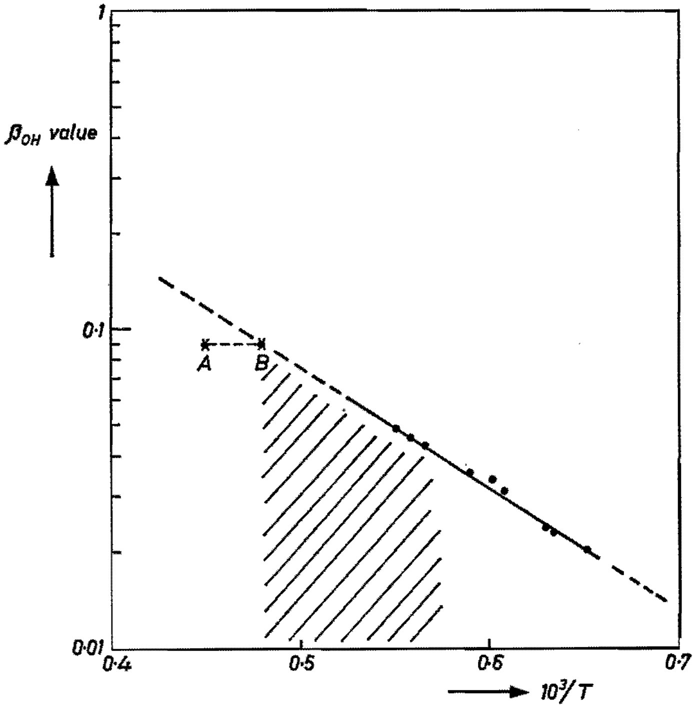

Fig. 3. β_{OH} as a function of reciprocal temperature, for samples treated in a hydrogen atmosphere. The shaded area indicates the temperature range where bubble growth could be detected when slowly cooling a melt.

point A, that this value is considerably lower than the extrapolated equilibrium β_{OH} value (about $120 . 10^{-3}$ mm^{-1}). When the sample is cooled down, the equilibrium OH concentration is reached at 1810 °C (point B). During further cooling, SiOH and SiH groups will react and physically dissolved hydrogen will be formed until local equilibrium pressure is reached. If the reaction is not frozen in, the H_2 pressure will exceed atmospheric pressure and bubble growth will take place.

Bubble-growth kinetics is proportional to the pressure difference

$$\Delta P = P_{\text{bubble}} - P_{\text{surrounding}}$$

and inversely proportional to the viscosity (η) of the medium in which the bubbles grow. During cooling, ΔP as well as η will increase. When η has become too high, bubble growth will stop. In fig. 3 the shaded area indicates the temperature range in which bubble growth could be detected.

At lower temperatures, long times for bubble growth are necessary. Therefore the diffusion out of the glass mass will become considerable and consequently the geometry of the melt will become an important factor.

When a melt is cooled down quickly, bubble formation can be prevented. It is not yet certain whether the failure of bubbles during rapid cooling is attributable to relatively low reaction kinetics or to low bubble-growth kinetics, or to both.

3.5. *Influence of the melting conditions on the thermochemical properties of the glass*

A bubble-free vitreous-silica sample was prepared by melting the raw material in a hydroxyl-free evacuated vitreous-silica ampoule, in an arrangement comparable with the arrangement used to melt the samples in an H_2/He atmosphere. Hydrogen and water were avoided during melting and the molybdenum melting crucible was protected by an argon atmosphere.

The sample was fired for 16 hours at 1050 °C in vacuum. The β_{OH} value of a sample thus treated was found to be $14{\cdot}6 . 10^{-3}$ mm^{-1}. The "stable" OH groups originate from the raw material itself [1]). When the sample was fired in an H_2 atmosphere the β_{OH} value increased. Table I gives the β_{OH} value after the various treatments of the sample. The amount of "stable" OH groups decreases a little after every heat treatment. This is probably due to a slow diffusion of molecular water out of the glass plate.

In the calculations made to determine the equilibrium constant K for reaction (2) the total OH concentration is taken into account and

$$x_{SiH} = x_{OH} - x_{OH}(\text{stable}),$$

$$x_{OH}(\text{stable}) = \tfrac{1}{2}\,(x_{OH}(\text{stable})\ \text{before reacting} + x_{OH}(\text{stable})\ \text{after reacting}).$$

TABLE I

consecutive treatments after melting in vacuum	β_{OH} value ($mm^{-1} . 10^3$)
16 hours 1050 °C/vacuum	15
16 hours 1550 °C/H_2	90
16 hours 1050 °C/vacuum	12
16 hours 1317 °C/H_2	54
16 hours 1050 °C/vacuum	10
16 hours 1390 °C/H_2	64
16 hours 1050 °C/vacuum	8

Figure 2 gives a plot of ΔG^0 as a function of the temperature (glass 2). The standard Gibbs-free-energy change differs slightly from the standard Gibbs-free-energy change for the same reaction with samples prepared in an H_2 atmosphere. The measurements are not accurate enough to enable one to determine whether this difference is to be attributed to an enthalpy and/or to an entropy effect. A possible explanation is that, contrary to the crystalline materials, the vitreous state is not defined exactly. The structure of the network on a molecular scale will be influenced by e.g. the preparation method. This is reflected in the physical properties of the glass and probably also explains the small difference in standard free-energy change for the reactions.

3.5. *Melting silica in an* He/H_2 (D_2)/H_2O (D_2O) *atmosphere*

The difference in stability between OH groups that are introduced according to reaction (2) or (4) can be used in order to demonstrate the existence of SiH centres as follows.

Vitreous-silica samples were prepared by melting the raw material in an H_2,H_2O,He atmosphere. The H_2,He mixture (H_2 50%, He 50%) was wetted by leading the gas through a water bath. The temperature of the water was held constant at 26 °C. The wetted gas was led through a vertically placed coiled condenser (length 1·5 m). The condenser was held at 21 °C. A dew point of 21 °C corresponds to a water partial pressure of 0·025 atmosphere. Table II gives the $\beta_{OH(OD)}$ values of the glass samples after the various treatments.

When during melting, at a time when it was sure that the melt was formed already, the composition of the gas mixture was changed (e.g. for 5 minutes), no perceptible change of the $\beta_{OH(OD)}$ values could be detected. This means that within the period of time that a melting experiment lasted, the exchange between the gases within the melt and the surrounding atmosphere was negligibly small. In an early stage of the sintering and melting processes the sur-

TABLE II

Values of β_{OH} and β_{OD}, before and after firing the same samples for 16 hours at 1050 °C in vacuum

sample no.	melting conditions				freshly molten		after 16 hours 1050 °C in vacuum	
	p_{H_2}	p_{D_2}	p_{H_2O}	p_{D_2O}	$\beta_{OH} \times 10^3$	$\beta_{OD} \times 10^3$	$\beta_{OH} \times 10^3$	$\beta_{OD} \times 10^3$
1	0·5	—	—	—	78	—	< 1	—
2	0·5	—	0·025	—	106	—	12·0	—
3	—	0·5	—	—	—	71	—	< 1
4	—	0·5	—	0·025	—	93	—	9

rounding atmosphere is enclosed between the grains and the mutual exchange between the gases in the melt and the surrounding atmosphere almost stops completely [1]). Therefore it is likely that the He/H_2 $(D_2)/H_2O$ (D_2O) ratio of the gas that is trapped by the sintering grains will have the same composition as the surrounding atmosphere.

The effect of water addition on the sintering properties of the raw material, and thus on the total amount of gases that is enclosed during melting, is not known quantitatively. Therefore it is not advisable to compare the β_{OH} values of samples 1 and 2 (or 3 and 4) directly. It is better to make use of the (apparent) difference in stability of the OH groups that are introduced according to reactions (2) and (4). When sample 1 was fired for 16 hours at 1050 °C under vacuum, the β_{OH} value was reduced to practically zero. When sample 2 was fired in the same way, the β_{OH} value was reduced to $12 \,.\, 10^{-3}$ mm^{-1}. This value decreased very slowly when the sample was fired for several hundreds of hours.

The ratio $OH_{stable}/OH_{unstable}$ (sample 2) is $12/94 = 0{\cdot}13$. The H_2O/H_2 ratio of the surrounding atmosphere is $0{\cdot}025/0{\cdot}49 \approx 0{\cdot}05$. When it is assumed that one H_2 molecule produces one OH and one SiH group the expected ratio between stable and unstable OH groups will therefore be 0·10, a value which is quite well in agreement with the experimental result (0·13).

In order to exclude the influence of small amounts of OH groups that are carried along with the raw material, D_2,D_2O,He mixtures were used (samples 3 and 4, table II).

Because of the fact that vitreous silica itself possesses a fairly strong absorption band in the 3·7-μm region the intensity of the OD absorption band was measured by placing an OD free sample of the same thickness in the reference beam of the spectrophotometer. The ratio $OD_{stable}/OD_{unstable}$ (sample 4) was 0·11, a value which is in agreement with the ratio (0·10).

4. Conclusions

(1) A linear relationship is observed between the equilibrium OH concentration and the square root of the hydrogen partial pressure.

(2) Hydrogen reacts with vitreous silica according to the reaction

$$2\,SiO_2 + H_2 \rightleftarrows \equiv SiOH + \equiv SiH\,.$$

In the temperature range between 1500 and 1800 °C the following relationship was found:

$$\Delta G^0 = 34500 + 14{\cdot}25\,T\ \text{(cal)}.$$

(3) When glasses are used which are prepared in completely different ways, the standard free-energy change for the reduction reaction may differ slightly.

(4) The IR-absorption data of samples prepared in a wetted and dry H_2 atmosphere support a reaction mechanism according to which an equimolar amount of $\equiv$SiOH- and $\equiv$SiH-like centres is formed during the reaction between H_2 and vitreous silica.

REFERENCES

[1] G. H. A. M. van der Steen and E. Papanikolau, Philips Res. Repts **30**, 103, 1975 (Part I of this thesis).

[2] G. H. A. M. van der Steen and E. Papanikolau, Philips Res. Repts. **30**, 192, 1975 (Part II of this thesis).

[3] N. C. Thombs and A. J. E. Welch, J. Iron and Steel Inst. **172**, 69, 1952.

[4] G. Grube and H. Spreidel, Z. Elektrochem. **43**, 339, 1949.

[5] H. F. Ramstadt and F. D. Richardson, Trans. Metallurgical Soc. AIME **221**, 1021, 1961.

[6] A. J. Moulson and I. P. Roberts, Trans. Faraday Soc. **57**, 1208, 1961.

[7] T. Bell, G. Hetherington and K. H. Jack, Phys. Chem. Glasses **3**, 141, 1962.

PART IV: REACTION AND DIFFUSION RATE CONTROLLED HYDROGEN TRANSPORT IN VITREOUS SILICA

Abstract

The concentration decay of "metastable" hydroxyl groups in vitreous silica has been studied as a function of temperature. Below 800 °C the rate of hydrogen evolution is controlled mainly by a reaction with a reaction rate constant

$$K_2 = f \exp(-63{\cdot}8\ \mathrm{kcal}/RT).$$

In the 1500 °C region H_2 transport is controlled by the diffusion of H_2 in vitreous silica in combination with the reaction

$$2\,SiO_2 + H_2 \rightleftarrows {\equiv}SiOH + {\equiv}SiH.$$

1. Introduction

Symbols used in this paper are:

A = unit area (cm^2)
B = $M_{H_2}\,\varrho/M_{SiO_2}$
C' = concentration of physically dissolved H_2 (g/cm^3)
C'' = concentration of chemically bonded H_2 (g/cm^3)
D = diffusion coefficient of H_2 in vitreous silica (cm^2/s)
H_t = amount of H_2 (g)
h = half the thickness of a vitreous silica plate (cm)
J_t = hydrogen transport (g/s)
K_e = equilibrium constant
K_1, K_2 = reaction rate constants (s^{-1})
M_{H_2} = 2·0 g/mole
M_{SiO_2} = 60·1 g/mole
P = hydrogen partial pressure (atm)
S = solubility of physically dissolved H_2 (g/cm^3 atm)
t = firing time (s)
x = OH mol fraction
x_0 = OH mole fraction at $t = 0$
x_h = OH mole fraction for $u = h$
$\bar{x}$ = mean OH mole fraction
x_{SiH} = SiH mole fraction
β_{OH} = optical density per mm (mm^{-1})
ε_{OH} = molar extinction coefficient, 58 litre/mole cm [1])
ϱ = 2·2 g/cm^3.

For the definition of u, a and b see figs 5a and b.

Hydroxyl groups can be introduced into vitreous silica by melting the raw material (crystalline quartz powder) in an H_2/He atmosphere [1]). OH groups are also formed when OH-free vitreous silica is heated in an H_2 atmosphere [2,3,4,5]). The most probable reaction that occurs is the following [6]):

$$2\,\mathrm{SiO_2} + \mathrm{H_2} \underset{K_2}{\overset{K_1}{\rightleftarrows}} \equiv\mathrm{SiOH} + \equiv\mathrm{SiH} \tag{1}$$

with

$$K_e = K_1/K_2 = (x \,.\, x_{\mathrm{SiH}})/P \,.\, (x_{\mathrm{SiO_2}})^2$$

and for

$$x = x_{\mathrm{SiH}}, \quad \text{and} \quad x \ll 1,\ K_e = x^2/P.$$

By heating a sample (thickness about 3 mm) at 1000 °C in vacuum the "metastable" OH groups disappear almost completely within a few hours. Below 500 °C the rate of the reaction

$$\equiv\mathrm{SiOH} + \equiv\mathrm{SiH} \xrightarrow{K_2} 2\,\mathrm{SiO_2} + \mathrm{H}_{2(\mathrm{phys.\ diss.})} \tag{2}$$

has become negligibly small. Only the physically dissolved hydrogen that is introduced into the glass during melting can be extracted from the samples at this temperature [7]). The present work is concerned with studying the rate-controlling processes for hydrogen transport (and formation) in vitreous silica in the temperature range between 500 and 1500 °C.

2. Experimental

2.1. *Samples*

Small differences in the chemical and physical properties can be expected between vitreous samples prepared in different ways [5]). In order to get an impression of the influence of the preparation method on the quantities determined in this paper, differently prepared samples were used:

Type I: Vitreous-silica samples prepared by melting milled Brazilian Rock crystals in an Mo crucible (inner diameter 25 to 40 mm) in an H_2 atmosphere and then quenching [1]). Plates of about 3 mm thickness were cut from the ingot and polished. The mean OH mole fraction of the samples thus prepared was $4{\cdot}7 \,.\, 10^{-4}$ ($\pm\, 0{\cdot}2 \,.\, 10^{-4}$).

Type II: Vitreous-silica tubes, produced by melting quartz powder in an H_2 atmosphere with continuous drawing. The mean OH mole fraction was $5{\cdot}6 \,.\, 10^{-4}$ ($\pm\, 0{\cdot}2 \,.\, 10^{-4}$).

Both types of samples proved to possess mainly "metastable" OH groups. The types are indicated in the figures.

2.2. *Infrared-absorption measurements*

The IR-absorption measurements were carried out with a Jasco-IRA 2 double-beam spectrophotometer. The optical density per mm (β_{OH}) at 2·73 μm is a relative measure of the hydroxyl concentration in the glass. The OH mole fraction was calculated as follows:

$$x = \frac{\beta_{\mathrm{OH}} \cdot M_{\mathrm{SiO_2}}}{\varepsilon_{\mathrm{OH}} \cdot \varrho \cdot 100}.$$

2.3. *Extraction experiments*

In order to remove OH groups and H_2, the samples were heated in vacuum or an argon atmosphere. The samples were brought into a hot oven and held in an argon atmosphere for one minute (this was the time estimated to be necessary to raise the sample to the temperature of the oven). Then the system was evacuated and the count off was started.

In the case where the samples were heated in a dry argon atmosphere the OH-concentration decay hardly differed from the vacuum-treated samples.

3. Results and discussion

3.1. *Reaction rate controlled H_2 production*

It is known from extraction experiment data that at 450 °C only physically dissolved hydrogen is removed from a sample [7]). The OH concentration, however, is hardly affected even when the sample is heated for several hundred hours. This would mean that the reaction rate constant (K_2) of reaction (2) is very low. At 650 °C it was possible to detect a decline in the OH concentration. The hydrogen formed as a result of reaction (2) diffuses out of the sample at a rate which is much higher than the rate of production [7]). Reaction kinetics therefore will describe the rate of the OH decay. When it is assumed that OH and SiH groups are present in equimolar amounts the following relationship holds:

$$-\frac{\mathrm{d}x}{\mathrm{d}t} = K_2\, x^2 \qquad \text{and} \qquad \frac{1}{x} = K_2\, t + \frac{1}{x_0}. \tag{4}$$

In fig. 1*a* typical plot is given of $1/x - 1/x_0$ as a function of firing time. When the rate of hydrogen production in the sample is controlled purely by

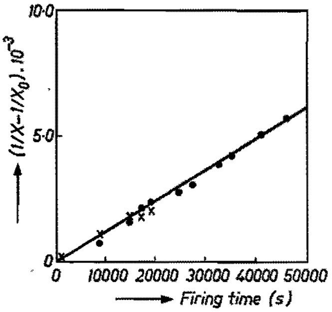

Fig. 1. ● Type-I sample, thickness 0·9 mm. × Type-I sample, thickness 3·03 mm. Firing temperature 710 °C.

reaction kinetics, the OH decay should be independent of the thickness of the sample. Two sample of 3·03 mm and 0·90 mm respectively were heated simultaneously at 710 °C in vacuum. $1/x - 1/x_0$ is plotted as a function of firing time in fig. 1. The best fitting lines through the measuring points almost coincide, which means that the OH decay is in fact independent of the thickness of the samples.

Another requirement that has to be fulfilled is the fact that the OH concentration should decrease homogeneously over the entire sample during the extraction. A sample with a thickness of 3·03 mm was heated at 710 °C until about half of the initial OH concentration was reached (sample ×, fig. 1). Thin layers were removed from one side of the sample by polishing. In fig. 2, $\bar{x}$ is given as a function of the thickness of the sample. No concentration profile could be detected.

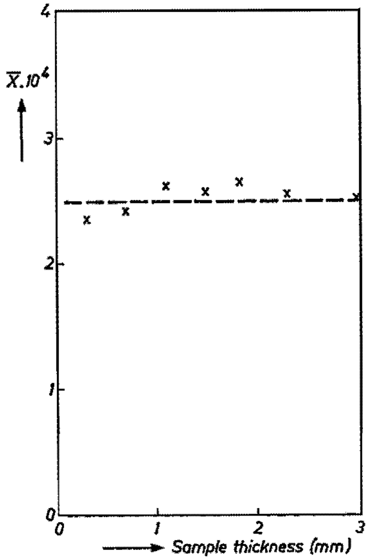

Fig. 2. Mean OH mole fraction ($\bar{x}$) as a function of the thickness of the sample (after firing for 19000 seconds at 710 °C, type I).

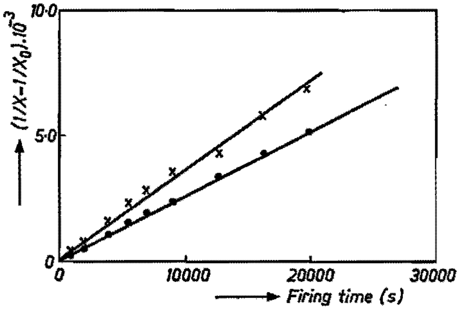

Fig. 3. ● Type-I sample, thickness 2·8 mm. × Type-I sample, thickness 1·75 mm. Firing temperature 810 °C.

When similar experiments were carried out at 810 °C a deviation from the model was found. The OH decay was no longer independent of the thickness of the sample (fig. 3). This indicates that the OH decay can no longer be described with reaction kinetics only.

3.1.2. Temperature dependence of K_2

The temperature dependence of K_2 was determined by analysis of the OH-concentration decay curves which were recorded at various temperatures. Log K_2 is plotted as a function of reciprocal temperature in fig. 4. From the slope of the straight portion of the curve it is calculated that

$$K_2 = f_2 \exp(-63800\ \text{cal}/RT) \text{ expressed in } s^{-1}. \qquad (6)$$

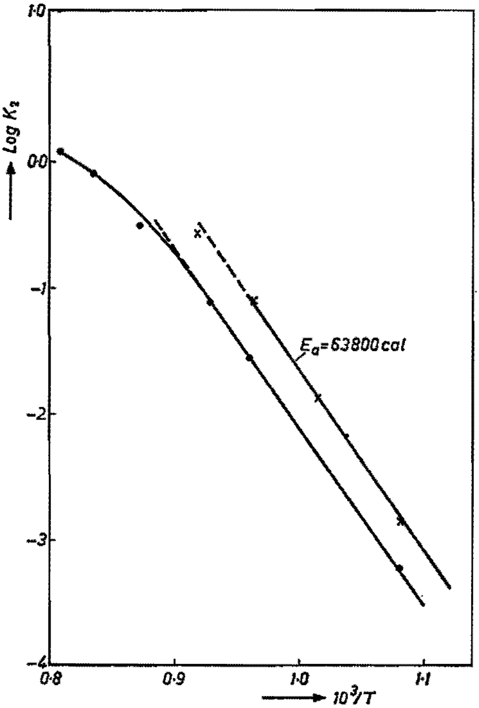

Fig. 4. Log K_2 as a function of reciprocal temperature. × Type I samples, thickness 2·8–3·1 mm. • Type II samples, thickness 1·5–1·7 mm.

with $f_2 = 2{\cdot}0 . 10^{12}\ s^{-1}$ and $7{\cdot}9 . 10^{11}\ s^{-1}$ for the type-I and type-II samples respectively. The reaction rate constant K_1 was calculated according to the relationship $K_1 = K_e . K_2$ with

$$K_e = 7{\cdot}5 . 10^{-4} \exp\left[-\left(\frac{34500 \pm 3000\ \text{cal}}{RT}\right)\right] \text{(ref. 5)} \qquad (7)$$

and therefore

$$K_1 = f_1 \ . \exp\left[-\left(\frac{98300 \pm 3000 \text{ cal}}{RT}\right)\right]. \tag{8}$$

The following reaction mechanisms may explain the values of the activation energies that were found:

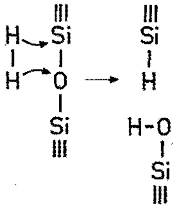

(9)

The strongest bond that has to be broken is the H–H bond with a bond energy of about 100 kcal/mole. This value is in quite good agreement with the activation energy that is found from the temperature dependence of K_1 namely 98·3 kcal/mole.

A rearranging reaction of the following type:

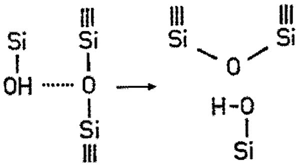

(10)

mobilizes the proton in the glass network. The proton will change its positions as long as an appropriate position is reached for reaction with an SiH partner. Whenever the proton change its position, an SiO bond must be broken. The energy needed to break a silicon–oxygen bond in glass will be somewhere between 50 and 100 kcal/mole [8,9,10]). The activation energy that is found from the temperature dependence of K_2 is 63·8 kcal/mole, a value which comes close to the bond-breaking energies of SiO.

3.2.1. Diffusion controlled hydrogen transport

It is fairly certain that, even at higher temperature (1000 °C), molecular hydrogen is the main diffusing species in vitreous silica. Hydrogen-ion transport may also occur but can be ignored [11,12]). Reacting OH and SiH groups, however, form the diffusing species namely molecular hydrogen. This fact has to be taken into account in the mathematical model that describes the rate of H_2 evolution (or the OH decay) during heating the glass in vacuum. In order to simplify the mathematical problem the following approximations were made:

(1) The sample is considered to be a semi-infinite plane sheet.
(2) Physically dissolved molecular hydrogen is the main diffusing species.

(3) The amount of H_2 present in the form of SiOH and SiH is large compared with the amount of physically dissolved hydrogen.

(4) The rate of reaction is high compared with the rate of out diffusion of H_2, and therefore chemical equilibrium will exist locally in the sample

$$2\,SiO_2 + H_2 \overset{K_e}{\rightleftarrows} \equiv SiOH + \equiv SiH \tag{11}$$

with

$$P = \frac{x^2}{K_e} \qquad (\text{for } x = x_{SiH} \ll 1). \tag{12}$$

(5) Henry's law is valid:

$$C' = S\,P. \tag{13}$$

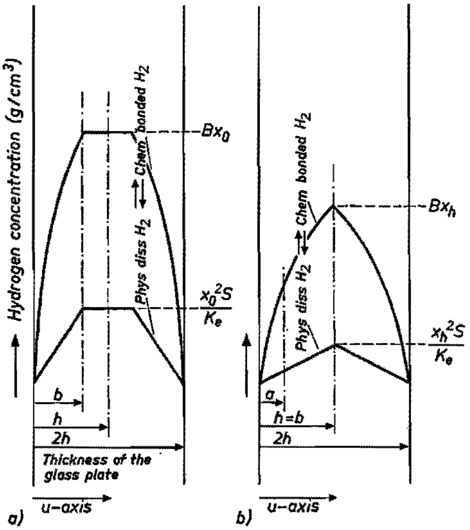

Fig. 5. Concentration profiles of physically dissolved and chemically bonded hydrogen in a vitreous-silica plate during extraction. *a)* before t^* is reached. *b)* after t^* is reached. (For explanation of the symbols see text.)

It can be shown that, when these conditions are fulfilled, the concentration profile of physically dissolved hydrogen (C') is made up of straight lines (trapezium fig. 5*a*, triangle fig. 5*b*).

In figures 5*a* and 5*b* the processes occurring during firing a sample in vacuum are shown in schematic form. The mathematical description of the OH decay can be found as follows: As long as the concentration profile of physically dissolved H_2 has the shape of a trapezium ($b \leqslant h$), point b (fig. 5*a*) will move as a function of time until $b = h$ ($t = t^*$). Within this period

$$C'' = B\,x_0\,(u/b)^{\frac{1}{2}} \qquad (\text{for } 0 \leqslant u \leqslant b) \tag{14}$$

and

$$C'' = B\,x_0 \qquad (\text{for } b < u \leqslant h). \tag{15}$$

The total amount of hydrogen present in a volume $A\,.\,h$ is

$$H_t = A \int_0^h C'' \,\mathrm{d}u \tag{16}$$

$$H_t = A\,B\,h\,x_0 - \tfrac{1}{3}\,A\,B\,b\,x_0. \tag{17}$$

The amount of H_2 leaving the sample per unit time is

$$J_t = A\,D\,\frac{\mathrm{d}C'}{\mathrm{d}u} = \frac{A\,D\,S\,x_0{}^2}{K_e\,b} \tag{18}$$

and

$$-\frac{\mathrm{d}H_t}{\mathrm{d}t} = J_t. \tag{19}$$

After combining eqs (17), (18) and (19) it is found that

$$b = \left(6\,\frac{x_0\,S\,D\,t}{K_e\,B}\right)^{\frac{1}{2}} \tag{20}$$

$$H_t = A\,B\,h\,x_0 - \tfrac{1}{3}\,A\,B\,x_0 \left(\frac{6\,x_0\,S\,D\,t}{K_e\,B}\right)^{\frac{1}{2}} \tag{21}$$

$$H_{t=0} = A\,B\,h\,x_0 \tag{22}$$

$$\frac{H_t/h}{H_{t=0}/h} = \frac{\bar{x}}{x_0} = 1 - \left(\frac{2\,x_0\,S\,D\,t}{3\,K_e\,B\,h^2}\right)^{\frac{1}{2}}. \tag{23}$$

This equation is valid until the time (t^*) is reached at which $b = h$ (eq. 19)

$$t^* = \frac{h^2\,K_e\,B}{6\,x_0\,S\,D} \tag{24}$$

$$\frac{\bar{x}_{(t=t^*)}}{x_0} = \tfrac{2}{3} \tag{25}$$

The OH decay is found for $t > t^*$ (b is a constant $= h$ and x_h is time dependent) in practically the same way.

$$\frac{\bar{x}}{x_0} = \frac{4}{9}\cdot\left(\frac{x_0\,S\,D\,t}{K_e\,B\,h^2} + 0{\cdot}5\right)^{-1} \quad \text{for } t > t^*. \tag{26}$$

$\bar{x}/x_0$ (eqs (23) and (26)) is a continuous monotonic decreasing function for all values of $t > 0$. The therm

$$\frac{x_0\,S\,D\,t}{K_e\,B\,h^2} \tag{27}$$

is present in eq. (23) as well as in eq. (26).

$\bar{x}/x_0$ was calculated as a function of this therm and plotted in fig. 6 (continuous line). The decay data were compared with the model as follows: Using numerical methods a value for $x_0\,D\,S/K_e\,B\,h^2$ was calculated so that the measuring points has the best fit with the curve in fig. 6. A typical plot of the

OH decay ($\bar{x}/x_0$) as a function of the therm (27) of a sample heated at 1415 °C is given in fig. 6. It is seen from this figure that the experimental results fit well with the model.

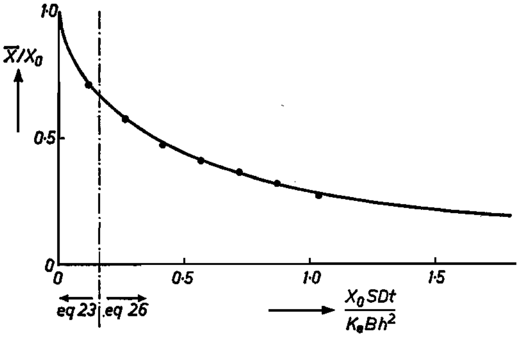

Fig. 6. The continuous curve is calculated (eqs (23) and (26)). Typical OH-concentration decay of a sample (type I) heated at 1415 °C in argon, with

$$\frac{x_0\ S\ D}{B\,K_e\,h^2} = 2{\cdot}8\ .\ 10^{-4}.$$

$D\ S/K_e$ was found when the constant B and the parameters x_0 and h were included. Numerical values of D, S and K_e were found elsewhere in the literature

$$D = 5{\cdot}65\ .\ 10^{-4}\ \exp\,(-10370/RT)\ \mathrm{cm^2/s}\ ^{13}) \qquad (28)$$

$$S = 2{\cdot}66\ .\ 10^{-7}\ \exp\,(1490/RT)\ \mathrm{g/cm^3\ atm}\ ^{13}) \qquad (29)$$

$$K_e = 7{\cdot}5\ .\ 10^{-4}\ \exp\left[-\left(\frac{34500 \pm 3000}{RT}\right)\right]\ ^{5}) \qquad (30)$$

and thus

$$D\ S/K_e = 2\ .\ 10^{-7}\ \exp\left(\frac{25620 \pm 3000}{RT}\right)\ \mathrm{g/cm\ atm}. \qquad (31)$$

Log $D\ S/K_e$ is plotted as a function of reciprocal temperature in fig. 7 (dash-dotted line).

The temperature dependence of the therm $D\ S/K_e$ was found experimentally by analysis of OH-decay curves, recorded at various temperatures, in the way described above. The experimental results are also plotted in fig. 7. It can be seen from this figure that, at temperatures higher than 1150 °C, the experimental data fit reasonably well with the values calculated according to the model. The change of sign of the activation energy is striking.

When samples were heated at temperatures higher than 1500 °C, they were recrystallized or considerably deformed and therefore we were unable to study the OH decay accurately in this temperature region.

In the temperature region between 800 °C and 1150 °C, H_2 evolution should be described by a mathematical model which takes reaction as well as diffusion kinetics into account.

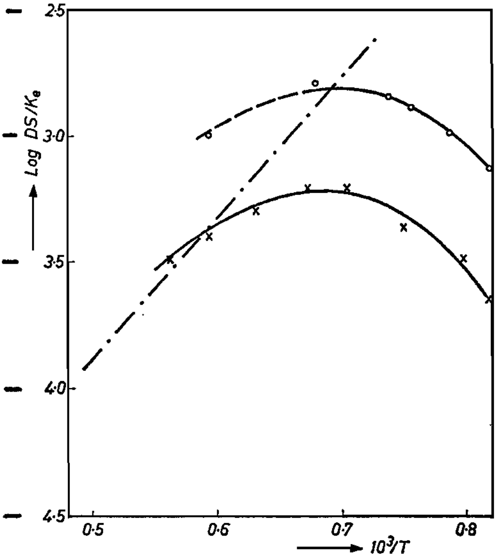

Fig. 7. Log $D\ S/K_e$ as a function of reciprocal temperature. o Type-I samples, thickness 2·8–3·1 mm. × Type-II samples, thickness 1·5–1·7 mm. The dash-dotted line was calculated according to eq. (31).

It should be noted that the temperature boundaries of this intermediate zone are strongly dependent on the geometry (thickness) of the sample as well as the initial OH concentration. The thinner the sample, the greater the extent by which the temperature hydrogen evolution is controlled by reaction kinetics only. The reason is to be found in the fact that gas transport by diffusion is strongly dependent on the thickness of the sample (cf. eqs (23) and (26)). The rate of production of H_2 as a result of reaction (2) is independent of the thickness of the sample.

3.2.2. Thickness dependence of the OH decay

It is seen from eqs (23) and (26) that the OH decay should be strongly dependent on the thickness of the sample. At a certain temperature the value of the therm $D\ S/K_e$ is constant. Two samples of various thickness were fired at the same temperature (1150 °C) and $D\ S/K_e$ was determined in the way described in the foregoing section. For a sample with a thickness of 5·81 mm a value of $1{\cdot}8\ .\ 10^{-3}$ g/cm atm was found for the therm $D\ S/K_e$ and a value of $1{\cdot}5\ .\ 10^{-3}$ g/cm atm was found for a sample with a thickness of 2·8 mm. This agreement is sufficient.

3.2.3. OH-concentration profiles

A 3·1 mm thick sample was fired at 1150 °C until the β_{OH} value was reduced to about half of its original value. The OH-concentration profile was determined as described in sec. 3.1.1. With the normal IR-absorption measurement techniques, only the mean OH concentration in a sample can be determined. $\bar{x}$ as a function of the thickness of the layer removed (a) was calculated as follows (cf. fig. 5*b*):

For $a \leqslant h$

$$\bar{x} = \frac{\int_a^h E \sqrt{u}\, \mathrm{d}u + \int_0^h E \sqrt{u}\, \mathrm{d}u}{2h - a} \tag{32}$$

$$\bar{x} = \frac{\frac{4}{3} E h^{\frac{3}{2}} - \frac{2}{3} E a^{\frac{3}{2}}}{2h - a} \tag{33}$$

and for: $2h > a > h$

$$\bar{x} = \frac{\int_0^{(2h-a)} E \sqrt{u}\, \mathrm{d}u}{2h - a} = \tfrac{2}{3} E (2h - a)^{\frac{1}{2}}, \tag{34}$$

E is a constant. E was calculated from relation (33) making use of the measured value of $\bar{x}$ ($2{\cdot}72 \,.\, 10^{-4}$) and for $a = 0$. This value for E was used to calculate the continuous line in fig. 8. In fig. 8 the experimental results are compared with the model.

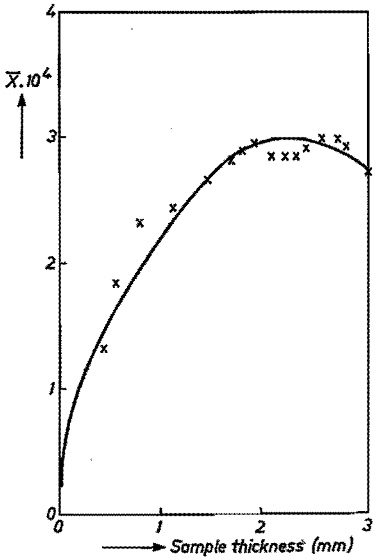

Fig. 8. Mean OH mole fraction as a function of the thickness of the sample, type I (after firing at 1150 °C).

4. Conclusions

(1) When OH containing vitreous-silica samples (OH groups originating from a reaction between H_2 and SiO_2 only) are heated in vacuum at temperatures below about 800 °C, the OH concentration decay is controlled by reaction kinetics. The reaction rate constant K_2 for the reaction

$$\equiv\text{SiOH} + \equiv\text{SiH} \underset{K_1}{\overset{K_2}{\rightleftarrows}} 2\,\text{SiO}_2 + \underset{\text{phys. diss.}}{\text{H}_2}$$

is $K_2 = f_2 \exp[-63800\,(\text{cal})/RT]$ and $K_1 = f_1 \exp[-98300\,(\text{cal})/RT]$. The frequency factor ($f$) in particular seems to be dependent on the technique of preparing the glass.

(2) At temperature higher than 1150 °C H_2 transport takes place mainly by diffusion of molecular hydrogen. The rate of removal of H_2 from the glass is not only a function of the diffusion coefficient and the thickness of the sample, but also of the (physical) solubility of H_2 in the glass, the equilibrium constant K_e and the initial OH concentration.

(3) Much confusion is found in the literature on the behaviour of hydroxyl as a result of a reaction between water and vitreous silica. The problems concerning the rate controlling processes for the introduction and removal of water in the glass are basically the same as for hydrogen in vitreous silica. Doremus [14]) has developed a model for the in-diffusion of water into vitreous silica which shows much resemblance to the model for H_2 transport in vitreous silica. How far one is justified in ignoring the hydrogen-ion mobility with respect to the mobility of molecular water in the glass, is not yet clear.

REFERENCES

[1]) G. H. A. M. van der Steen and E. Papanilokau, Philips Res. Repts **30**, 103, 1975 (Part I of this thesis).
[2]) S. P. Faile and D. M. Roy, Mat. Res. Bull. **5**, 385, 1970.
[3]) S. P. Faile and D. M. Roy, J. Amer. ceram. Soc. **54**, 533, 1971.
[4]) T. Bell, G. Hetherington and K. H. Jack, Phys. Chem. Glasses **3**, 141, 1962.
[5]) G. H. A. M. van der Steen, Philips Res. Repts **30**, 309, 1975 (Part III of this thesis).
[6]) G. H. A. M. van der Steen and H. van den Boom, (Part V of this thesis).
[7]) G. H. A. M. van der Steen and E. Papanikolau, Philips Res. Repts **30**, 192, 1975 (Part II of this thesis).
[8]) H. Scholze, Glas, F. Vieweg und Sohn (eds), Braunschweig, 1965.
[9]) I. Náray-Szabó and J. Ladik, Nature **188**, 226, 1960.
[10]) E. W. Sucov, J. Amer. ceram. Soc. **46**, 14, 1963.
[11]) P. F. Jorgensen and F. J. Norton, Phys. Chem. Glasses **10**, 23, 1969.
[12]) R. W. Lee, J. Chem. Phys. **38**, 448, 1963.
[13]) R. W. Lee, R. C. Frank and D. E. Swets, J. Chem. Phys. **36**, 1062, 1962.
[14]) R. H. Doremus, Reactivity of solids, Mitchell, De Vries, Roberts and Cannon (eds), Wiley & Sons, 1969, p. 667.

PART V: RAMAN SPECTROSCOPIC STUDY OF HYDROGEN-CONTAINING VITREOUS SILICA

Abstract

It is shown by Raman spectroscopy that high-temperature hydrogen-impregnated vitreous silica contains, in addition to physically dissolved hydrogen, $\equiv$SiOH and $\equiv$SiH groups.

A Raman-scattering peak with a wave number shift of 3685 cm^{-1} was assigned to the OH stretching vibration, a peak with a wave number shift of 2254 cm^{-1} to a SiH stretching vibration and a peak with a wave number shift of 4135 cm^{-1} to the presence of physically dissolved hydrogen. When hydrogen was replaced by deuterium, appropriate shifts of the peaks mentioned were found.

1. Introduction

Two different methods are known for introducing hydrogen in the form of OH groups into vitreous silica, namely:

(a) a reaction between water and vitreous silica

$$H_2O + 2\,SiO_2 \rightarrow 2 \equiv SiOH, \qquad (1)$$

(b) a reaction between hydrogen and vitreous silica

$$H_2 + 2\,SiO_2 \rightarrow \equiv SiOH + \equiv SiH. \qquad (2)$$

Hitherto it has been impossible to find any clear direct proof of the existence of SiH in glass. If the existence of SiH, however, was assumed, it would be easy to explain one or two phenomena, for instance

(1) The relationship

$$P_{H_2} = K\,.\,[OH]^2$$

has been found experimentally [1]) and is consistent with reaction mechanism (2).

(2) The thermal stability of the OH groups formed according to reaction (2) is less than the thermal stability of the OH groups that are formed according to reaction (1). Reaction-(2) OH groups are compensated by an equal amount of SiH groups which may explain the "stability" difference.

(3) The molar extinction coefficient (ε_{OH}) for hydroxyl in vitreous silica has been determined by Stephenson and Jack [2]). They related the weight loss of "water"-containing vitreous silica (Spectrosil) to the changes of the optical density at 3685 cm^{-1}. A value of 78 l $mole^{-1}$ cm^{-1} was found for ε_{OH}. Hydrogen evolution of "hydrogen"-containing vitreous silica has been studied before [3]). When it is assumed that only half of the hydrogen atoms are present in the form of Si–OH and the other half in the form of Si–H, a value of 58 l $mole^{-1}$ cm^{-1} is found. This value is quite close to the results of Stephenson

and Jack. If it were assumed that the H_2 molecule produces two OH groups and a reduced silicon atom, the extinction coefficient would be 29 l mole^{-1} cm^{-1}.

An SiH stretching vibration is expected to occur at frequencies of about 2250 cm^{-1} [4]). Vitreous silica itself possesses an IR-absorption band in this region [5,6]). This absorption band hampers accurate study of SiH centres, using IR-absorption methods [6]).

There are indications, however, that under certain circumstances SiH groups are formed. Faile and Roy [7]), for instance, found an enhanced intensity of the 2250-cm^{-1} absorption band in hydrogen-impregnated irradiated glasses.

Beckmann and Harrick [8]) investigated thin SiO_2 layers (2000 Å), thermally grown on a silicon plate, with the aid of internal reflection spectroscopic methods. They also recorded a band at 2250 cm^{-1} which they attributed to the presence of SiH centres.

The infrared and Raman activity of vibrations in general will be different. Raman-spectroscopic data, given in this paper, will show that under certain circumstances considerable amounts of SiH centres may be present in vitreous silica. The infrared activity of the SiH stretching vibration proves to be low (not detectable) compared with the Raman activity.

2. Experimental

2.1. *Description of the vitreous-silica samples*

Five vitreous-silica samples were prepared. Each of the five samples will differ from the other samples with respect to hydrogen economics. The differences were introduced by melting the samples under different conditions or by an additional heat treatment. The characteristic property of each sample will be mentioned.

Sample A was prepared by melting quartz powder in a Mo crucible in an H_2 atmosphere [9]). It is assumed that this sample will contain SiOH, SiH as well as physically dissolved hydrogen.

Sample B was prepared by heating sample A for 48 hours under vacuum at 450 °C. At 450 °C, physically dissolved H_2 can be extracted from the sample without affecting the SiOH and SiH concentration [3]).

Sample C was prepared by heating sample A for 24 hours under vacuum at 1000 °C. At 1000 °C SiOH and SiH groups will react to physically dissolved hydrogen which diffuses out of the sample [10]). This sample therefore is assumed to be "empty" with respect to hydrogen.

Sample D was prepared by flame spraying of the quartz powder in an H_2/O_2 flame. The sample was heated for 24 hours in vacuum. This sample will contain "stable" OH groups that cannot be removed by the above mentioned additional heat treatment. SiH groups as well as physically dissolved H_2 are not expected to be present in the sample.

Sample E was prepared by melting quartz powder in a D_2 atmosphere. This sample is assumed to contain SiOD, SiD and D_2.

Plates (size about 10×5×3 mm) were cut from the glass specimens and polished to optical flatness. Each plate had four faces polished in such a way that one set of two parallel polished faces were perpendicular to another set of two parallel faces so as to permit Raman measurements.

The optical density per mm at 3685 cm^{-1} (β_{OH} value) was measured with a Jasco IRA-2 spectrophotometer. The β_{OH} value is a relative measure of the hydroxyl concentration in the vitreous-silica sample (table I). The intensity of the 2250-cm^{-1} absorption band was studied carefully for all samples, but no significant differences could be found.

TABLE I

sample	wave numbers (cm^{-1})			β_{OH} value (mm^{-1})
	2254	3685	4135	
A	s	w — m	w — m	91 . 10^{-3}
B	s	w — m	—	91 . 10^{-3}
C	v.w.	—	—	1 . 10^{-3}
D	—	m	—	150 . 10^{-3}
	1629	2720	2975	β_{OD} value (mm^{-1})
E	s	w — m	w — m	70 . 10^{-3}

where: s = strong, m = medium, w = weak and v.w. = very weak.
The intensity is compared with the 1595-cm^{-1} silica peak.

2.2. *Raman-scattering measurements*

The Raman spectra were measured by excitation of the samples with an Argon ion laser (Coherent Radiation model 52) operating at a wavelength of 4880 Å. The power on the sample was about 600 mW. The measurements were done in a 90° scattering arrangement in a modified Steinheil–Lear Siegler optical set-up and the scattered radiation was analysed with the aid of a Jarall–Ash 25–100 dual monochromator. The samples were positioned in the exciting beam with all polished faces perpendicular to the optical plane formed by the excitation direction and the direction in which the scattered radiation was collected. The signal, detected by an ITT-FW 130 photomultiplier, was DC amplified and recorded on a strip chart recorder. All measurements were carried out at room temperature.

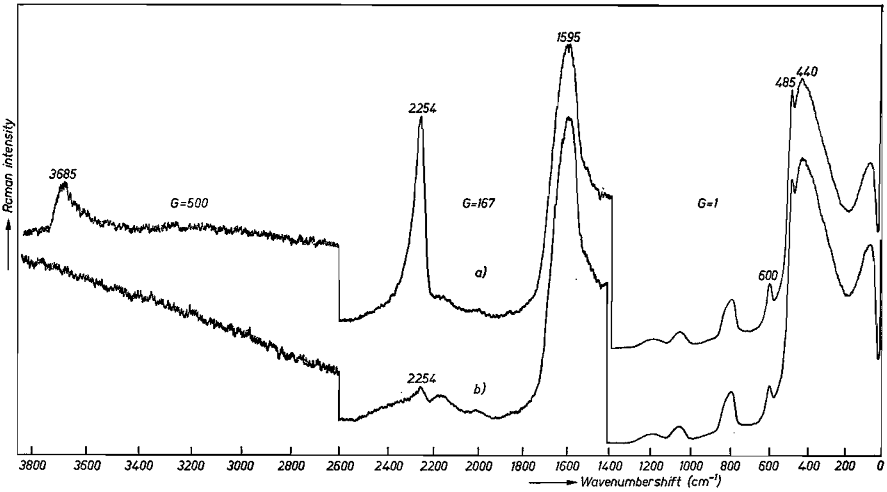

Fig. 1. Raman spectra of sample A(*a*) and sample C(*b*) (plates 10×5×3 mm). Excitation 4880 Å, 600 mW, with polarization scrambler. Scanning rate 4 cm^{-1} s^{-1}; time constant 0·5 s; slit width 10^{-1} to 1400 cm^{-1}. Above 1400 cm^{-1} scanning rate: 0·4 cm^{-1} s^{-1}; time constant 5 s; voltage employed with dc detection was 1600 V over the entire range. Overall gain setting (G) as indicated.

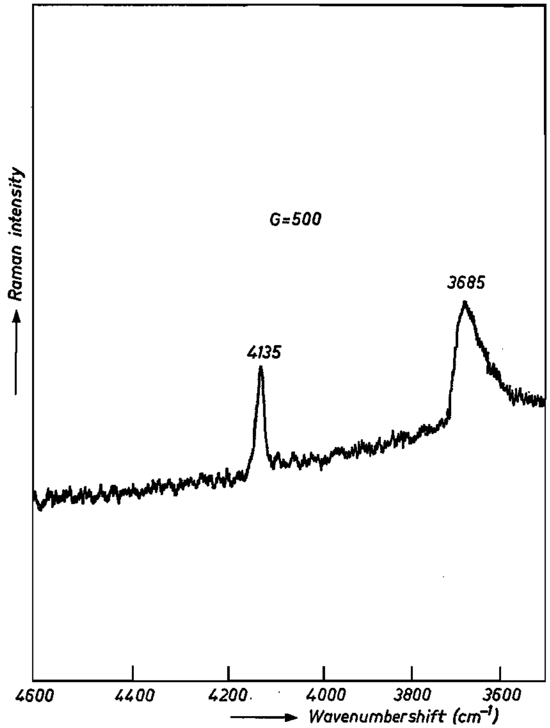

Fig. 2. Raman spectrum of sample A. Excitation 4880 Å, 600 mW, with polarization scrambler. Scanning rate 0·4 cm^{-1} s^{-1}; time constant 5 s; slit width 10 cm^{-1}. Overall gain setting (G) as indicated. The spectrum of sample C is not shown because this does not show peaks at all.

3. Results and discussion

In order to assign the relevant Raman peaks to the most probable vibration the following deduction method was used:

(a) The spectra of sample A and C were compared. Sample A is assumed to contain SiOH, SiH and physically dissolved H_2. In sample C no hydrogen is expected to be present. The spectrum of sample A showed three peaks at 2254, 3685 and 4135 cm^{-1} that were not present (or only to a limited extent) in the spectrum of sample C (cf. fig. 1*a*, *b* and 2). These peaks therefore are assigned to H-containing centres.

(b) The only difference between the spectra of samples A and B is the fact that the 4135-cm^{-1} peak is not present in the spectrum of sample B. Physically dissolved hydrogen is removed from sample B during extraction at 450 °C. The 4135-cm^{-1} peak therefore, is assigned to physically dissolved hydrogen or the presence of hydrogen in (sub) microscopically small bubbles. The recorded frequency is in good agreement with the H–H stretching vibration [11]).

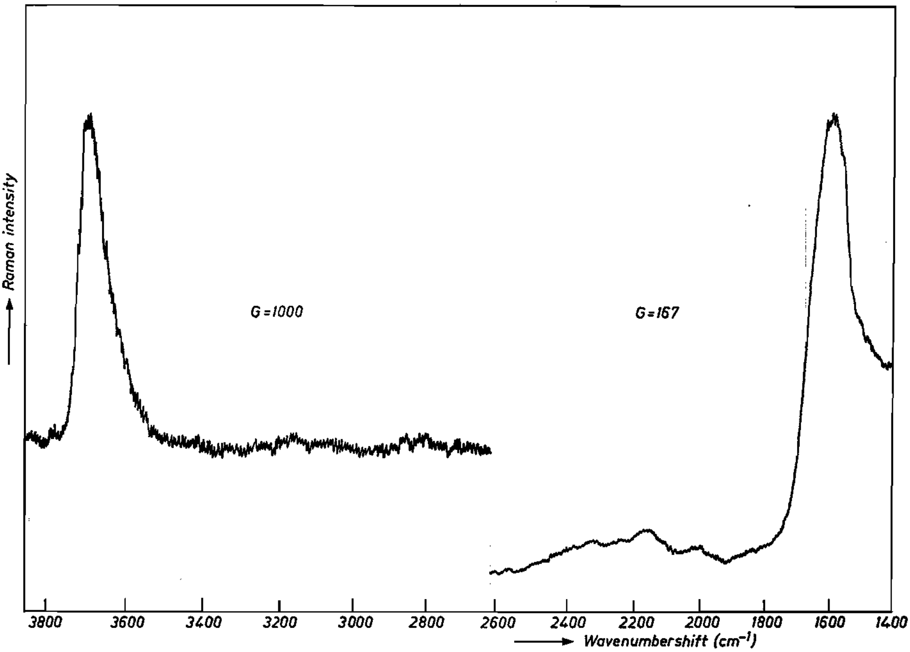

Fig. 3. Raman spectrum of sample D. Excitation 4880 Å, 600 mW, with polarization scrambler. Scanning rate 0·4 cm^{-1} s^{-1}; time constant 5 s; slit witdh 10 cm^{-1}. Overall gain setting (G) as indicated.

(c) The 3685-cm^{-1} peak was present in all OH-containing samples (A, B, D, figs 1*a* and 3). The intensity of this peak varies with the OH concentration (table I). The recorded frequency is in agreement with the OH stretching vibration [12]).

(d) The 2254-cm^{-1} peak is present in the spectra of samples A and B, but not in the spectrum of sample D although the hydroxyl content is of the same order of magnitude in those samples. This peak is assigned therefore to SiH groups which are assumed to occur in samples A and B. The recorded frequency is in agreement with a Si–H stretching vibration [4]).

The assignments can be readily checked in our case by replacing hydrogen by deuterium. The frequency of a vibrational motion between two atoms can be expressed in the form:

$$\nu = K\sqrt{\frac{F}{\mu}}$$

where: ν = fundamental vibration frequency,
F = force constant,
μ = reduced mass.

When hydrogen is replaced by deuterium, the following relationship is obtained:

$$\nu_D = \sqrt{\frac{\mu_{XH}}{\mu_{XD}}} \cdot \nu_H$$

where: X = Si, O, H or D.

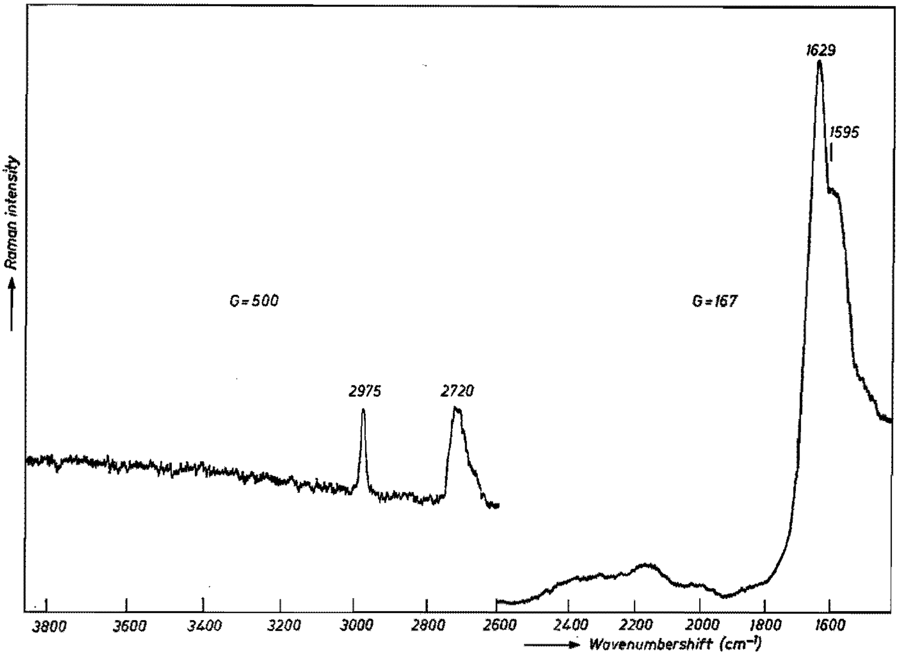

Fig. 4. Raman spectrum of sample E. Excitation 4880 Å, 600 mW, with polarization scrambler. Scanning rate 0·4 cm^{-1} s^{-1}; time constant 5 s; slit width 10 cm^{-1}. Overall gain setting (G) as indicated.

The spectrum of the deuterized sample E is given in fig. 4. In table II the calculated values and the recorded frequencies are compared. The calculated values are in good agreement with the experimental results.

TABLE II

frequency (cm^{-1})		assignment
calculated	recorded	
2681	2720	OD
1621	1629	SiD
2924	2975	D_2

4. Conclusions

High-temperature hydrogen-impregnated vitreous silica contains in addition to physically dissolved H_2, SiOH and SiH groups. All three centres proved to be Raman active. The 2254-cm^{-1} scattering peak was assigned to the SiH stretching vibration, the 3685 cm^{-1} peak to the OH stretching vibration and the 4135 cm^{-1} peak to the H–H stretching vibration. In a deuterium-impregnated sample a corresponding shift of above-mentioned Raman peaks was found.

REFERENCES

¹) G. H. A. M. van der Steen, Philips Res. Repts **30**, 309, 1975 (Part III of this thesis).

²) G. W. Stephenson and K. H. Jack, Trans. Brit. ceram. Soc. **59**, 397, 1960.

³) G. H. A. M. van der Steen and E. Papanikolau, Philips Res. Repts **30**, 192, 1975 (Part II of this thesis).

⁴) C. Morterra and M. J. D. Low, J. Phys. Chem. **73**, 327, 1969.

⁵) R. V. Adams and R. W. Douglas, J. Soc. Glas Techn. **43**, 147 T.

⁶) W. A. Pliskin, in Semiconductor Silicon 1973, H. R. Huff and R. R. Burgess (eds), Electrochem. Soc. **00**, 000, 1900.

⁷) S. P. Faile and R. M. Roy, Mat. Res. Bull. **5**, 385, 1970.

⁸) K. H. Beckman and N. J. Harrick, J. electrochem. Soc. **118**, 615, 1971.

⁹) G. H. A. M. van der Steen and E. Papanikolau, Philips Res. Repts **30**, 103, 1975 (Part I of this thesis).

¹⁰) G. H. A. M. van der Steen, (Part IV of this thesis).

¹¹) G. Herzberg, Molecular spectra and molecular structure, I. Spectra of diatomic molecules, 2nd Edition, D. Van Nostrand Company inc., New York, 1950.

¹²) G. E. Walrafen and J. Stone, Appl. Spectroscopy **29**, 337, 1975.

Curriculum vitae

Gerardus Henricus Antonius Maria van der Steen werd op 8 juli 1943 te Tilburg geboren. De middelbare avondschoolopleiding die hij aan het Odulphus Lyceum te Tilburg ontving, werd met het behalen van het einddiploma HBS-B in 1963 afgesloten. Na het vervullen van zijn militaire dienstplicht trad hij in 1965 in dienst van het Natuurkundig Laboratorium van de N.V. Philips' Gloeilampenfabrieken.

In het jaar 1969 liet hij zich inschrijven als student aan de Technische Hogeschool Eindhoven, afdeling Scheikundige Technologie. In 1972 werd hij in staat gesteld om een jaar lang full-time te gaan werken aan zijn afstudeeronderzoek dat hij uitvoerde onder leiding van Prof. Dr. G. C. A. Schuit in de groep Anorganische Chemie.

Na het behalen van zijn ingenieursdiploma (januari 1973) keerde hij terug naar de N.V. Philips' Gloeilampenfabrieken, waar hij tot op heden werkzaam is in de groep Glasontwikkeling en Applikatie welke onder leiding staat van Dr. Ir. A. Kats en onderdeel vormt van het Ontwikkelingscentrum Glas onder leiding van Dr. W. Verweij.

Het experimentele werk dat in deze dissertatie wordt beschreven, is uitgevoerd in de periode 1973–1975.

STELLINGEN

bij het proefschrift van

G. H. A. M. van der Steen

6 april 1976
T.H. Eindhoven

I

Het is niet geoorloofd om diffusiecoëfficiënten voor waterstof en water in kwartsglas te berekenen uit de concentratieprofielen van een van de reactieprodukten (OH-groepen) zonder de reactie tussen waterstof en water en het glas in de berekeningen te betrekken.

T. Drury and J. P. Roberts, Phys. Chem. Glasses **4**, 79, 1963.
T. Bell, G. Hetherington and K. H. Jack, Phys. Chem. Glasses **3**, 141, 1962.

II

De intensiteit van de 2·73 μm infrarood absorptieband mag niet zonder meer worden gebruikt om de concentratie van chemisch gebonden waterstof in kwartsglas te bepalen.

G. H. A. M. van der Steen and E. Papanikolau, Philips Res. Repts **30**, 192, 1975.

III

Het is onwaarschijnlijk dat voor toevoeging van kleine hoeveelheden alkali en aard-alkali metalen het watergehalte van kwartsglas verlaagd zal worden.

Auslegeschrift 2.205.560, R. Brünig, Heraeus-Schott Quarzschmelze G.m.b.H. (1974).

IV

Het is onwaarschijnlijk dat er een correlatie bestaat tussen de intensiteiten van de 485 cm^{-1}, 600 cm^{-1} en 3685 cm^{-1} Raman verstrooiingspieken in kwartsglas.

G. E. Walrafen and J. Stone, Appl. Spectr. **29**, 337, 1975.

V

Tijdens het zogenaamde presulfideren van MoO_3-houdende katalysatoren wordt de katalytisch actieve substantie MoS_2 gevormd.

VI

De interpretatie van de metingen aan magnetisch verdunde systemen kan worden bemoeilijkt door clustervorming en/of een inhomogene verdeling van de te onderzoeken ionen.

VII

Het afschatten van thermische energieën die bij een reactie een rol spelen m.b.v. dissociatie-energieën kan tot grote fouten leiden.

T. Bell, G. Hetherington and K. H. Jack, Phys. Chem. Glasses 3, 141, 1962.

VIII

De mate van complexiteit van een model of mechanisme dat een proces beschrijft is niet alleen afhankelijk van de relevante fysische grootheden maar ook van de fantasie van de ontwerper.

IX

Scheikundigen, natuurkundigen en wiskundigen hebben bij de uitoefening van hun respectievelijke beroepen, minder last van de publieke opinie dan economen en sociologen.

X

Statistische gegevens, voorzien van een eigen interpretatie, zijn een geliefd wapen van politici.

XI

De objectiviteit van de weergave van feiten en gebeurtenissen kan worden benadeeld door het polariserende effect van een politieke stellingname.

XII

De berichtgeving en commentaren over economische gebeurtenissen kunnen een katalytische uitwerking hebben op deze gebeurtenissen.

XIII

Niet alleen het streven naar sociale rechtvaardigheid maar ook afgunst werkt nivellerend.